CHALMERS
UNIVERSITY OF TECHNOLOGY

Effect of Strength Enhancer Admixtures on Carbonation Resistance of Concrete

Master's thesis in the Master's Programme Structural Engineering and Building Technology

GABRIEL ARONSSON
ARCHANATH DICKWELLA

DEPARTMENT OF ARCHITECTURE AND CIVIL ENGINEERING

CHALMERS UNIVERSITY OF TECHNOLOGY
Gothenburg, Sweden 2025
www.chalmers.se

MASTER'S THESIS ACEX30

Effect of Strength Enhancer Admixtures on Carbonation Resistance of Concrete

Master's Thesis in Structural Engineering
and Building Technology

GABRIEL ARONSSON
ARCHANATH DICKWELLA

CHALMERS
UNIVERSITY OF TECHNOLOGY

Department of Architecture and Civil Engineering
Division of Building Technology
CHALMERS UNIVERSITY OF TECHNOLOGY

Gothenburg, Sweden 2025

Effect of Strength Enhancer Admixtures on Carbonation Resistance of Concrete

Master's Thesis in Structural Engineering and Building Technology

GABRIEL ARONSSON

ARCHANATH DICKWELLA

Examensarbete ACEX30
Institutionen för arkitektur och
samhällsbyggnadsteknik Chalmers tekniska
högskola, 2025

Department of Architecture and Civil Engineering
Division of Building Technology
Chalmers University of Technology
SE-412 96
Göteborg Sweden
Telephone: + 46 (0)31-772 1000

Effect of Strength Enhancer Admixtures on Carbonation Resistance of Concrete

Master's thesis in Structural Engineering and Building Technology

GABRIEL ARONSSON

ARCHANATH DICKWELLA

Department of Architecture and Civil Engineering
Division of Building Technology
Chalmers University of Technology

ABSTRACT

Supplementary Cementitious Materials (SCMs) have been used when mixing concrete to minimize the amount of Portland cement. This may lead to a decreased carbonation resistance, which in turn leads to risk for corrosion in reinforcement and poor mechanical performance and durability. In recent years, Strength Enhancing Admixtures (SEAs) have been used to enhance both the early and later age strength of concrete. It is however a new field of how they impact the carbonation resistance of concrete using SCMs.

This study analyzed the effect of using strength enhancing admixtures on carbonation when using volcanic pozzolans and iron silicates as SCMs in concrete. For this, accelerated carbonation testing was performed according to the standard SS-EN 12390-12:2020 with a carbon dioxide concentration of 3%. Compressive strength testing (according to standard SS-EN 196-1:2016) and capillary absorption testing (according to standard NT Build 368,1991) was also carried out to study how the carbonation affects the mechanical performance and durability when using SEAs. The SEAs used were Master X-Seed STE53 and Master X-Seed 100. To be able to assess the effect of the SEAs, concrete mixes with varying dosages of SEA were prepared alongside mixes containing no SEA to compare the results to.

The results show that the studied SEAs have a positive impact on the carbonation resistance in concrete utilizing pozzolans and iron silicates as SCMs. The effects were especially pronounced in the case of iron silicates. Compressive strength and capillary absorption were also affected positively, with the SEAs generally yielding an increase in 28 days and 56 days compressive strength, and an increased resistance to capillary water ingress. When comparing the two different SEAs, it was shown that Master X-Seed STE53 had a greater impact on reducing the carbonation rates.

Keywords: accelerated carbonation, strength enhancing admixtures, iron silicates, VPI, compressive strength, capillary absorption, Akmenes, Bascement

Acknowledgements

We would like to express our sincere gratitude to our Examiner, Arezou Baba Ahmadi, for arranging this study in collaboration with Thomas Betong and helping us throughout the study. We are deeply grateful to our academic supervisor, Helen Jansson, for her continuous support and insightful guidance, which strengthened the quality of this work on countless occasions. We also extend our heartfelt thanks to our industrial supervisor at Thomas Betong, Ingemar Löfgren, for his sustained support during specimen preparation, testing and results analysis, and for giving us the autonomy and time to work independently in the laboratory. Finally, we thank Oskar Esping at Thomas Betong for his valuable insights during planning and his hands-on assistance with specimen preparation.

Gabriel Aronsson & Archanath Dickwella,
Gothenburg, 2025

Table of Contents

Abbreviations

Ak	Akmenes Cement
Al_2O_3	Aluminium Oxide
ASR	Alkali-Silica Reaction
BAS	Bascement Cement
$CaCO_3$	Calcium Carbonate
CaO	Calcium Oxide
$Ca(OH)_2$	Calcium Hydroxide (Portlandite)
Ca/Si	Calcium to Silicon Ratio
CH	Calcium Hydroxide
CO_2	Carbon Dioxide
C-S-H	Calcium Silicate Hydrate
GGBS	Ground Granulated Blast-furnace Slag
IS	Iron Silicate
MgO	Magnesium Oxide
RH	Relative Humidity
SCM	Supplementary Cementitious Material
SEA	Strength Enhancing Admixture
SiO_2	Silicon Dioxide
VPI	Volcanic Pozzolana Iceland
w/b	Water to Binder Ratio
w/c	Water to Cement Ratio
XRF	X-Ray Fluorescence

List of Tables

List of Figures

Introduction

Concrete structures are often exposed to environmental conditions that can compromise their long-term durability. Out of all the durability degradation processes, carbonation is one of the most common and significant issues. It is the process by which atmospheric carbon dioxide (CO_2) permeates through the concrete and reacts with calcium hydroxide ($Ca(OH)_2$) to form calcium carbonate ($CaCO_3$), leading to a reduction in alkalinity which may cause corrosion of the embedded reinforcing steel [1]. Carbonation is controlled by different variables that cover porosity, permeability, curing conditions, as well as the cementitious matrix composition.

In order to enhance durability and minimize Portland cement content, Supplementary Cementitious Materials (SCMs) including fly ash, ground granulated blast furnace slag (GGBS), and volcanic pozzolans have been widely used [2]. They have an impact on the chemical composition and microstructure of the concrete, tending to produce denser matrices but, in some instances, decreased resistance to carbonation due to limited $Ca(OH)_2$ availability [3].

In the last decades, strength-enhancing admixtures (SEAs) have appeared as a type of chemical additive with the target of enhancing the mechanical performance of the concrete, both early and later age strength. Nevertheless, their impact on the carbonation resistance of the concrete, primarily in combination with SCMs, is still a new field of research. Previous studies have indicated that while matrix densification due to SCMs can offer durability benefits, the effects on carbonation resistance are not always consistent and may vary depending on the specific mix composition [4]. This research explores the combined impact of SCMs and SEAs on the carbonation resistance of concrete, specifically by comparing a pozzolanic cementitious system with Iron Silicate.

1.1. Background

1.1.1. Mechanisms affecting concrete durability

The durability of concrete can be weakened by a variety of degradation processes. Among the most prevalent durability issues are carbonation, ingress of chlorides, sulfate attack, freeze-thaw damage, alkali-silica reaction (ASR), and leaching. They can contribute to alkalinity loss, corrosion of embedded reinforcement, cracking, and overall degradation of mechanical properties [2]. For example, carbonation decreases the pH of the pore solution, in turn initiating corrosion of steel when the passive coating is damaged [1]. In the same way, chloride ingress, especially in coastal environments or in the case of the use of de-icing salt, leads to premature corrosion of reinforcement [5]. ASR, an interaction of alkali hydroxides of the cement with reactive silica from aggregates, leads to formation of expansive gel and cracking [6]. All of these durability issues serve as evidence of the need for mix design, classification of environmental exposure, and proper use of materials and admixtures in order for the lifetime of concrete to be improved [7].

1.1.2. Carbonation and its effect on concrete

Carbonation is a process where CO_2 from the air moves into the concrete's pore system and reacts mainly with $Ca(OH)_2$ in the cement paste. First, CO_2 dissolves in the pore water to form carbonic acid, and then this acid reacts with hydration products, reducing the concrete's pH [8,9]. While $Ca(OH)_2$ is the main target, other phases like parts of the Calcium Silicate Hydrate (C-S-H) gel can also carbonate over time.

The carbonation reaction in concrete primarily involves CO_2 reacting with $Ca(OH)_2$ to form $CaCO_3$ and water, as stated in Equation (1):

$$CO_2 + Ca(OH)_2 \rightarrow CaCO_3 + H_2O \qquad (1)$$

In this chemical reaction process, CO_2 from the atmosphere reacts with $Ca(OH)_2$, a product of cement hydration, to form $CaCO_3$, which precipitates in the pore structure, and water (H_2O).

The rate at which carbonation happens depends on how easily CO_2 can move through the pores and how much Calcium-included material, $Ca(OH)_2$ and C–S–H, is available [1,10] Factors like concrete porosity, surrounding CO_2 levels, temperature, and especially relative humidity (RH) all become decisive. Carbonation happens fastest when RH is around 60–70%, because the concrete has just enough moisture for chemical reactions, but not so much that CO_2 diffusion slows down [10]. In contrast, if the concrete is too dry or fully saturated, carbonation slows down. In very dry concrete, carbonation is barely existent because the reaction requires moisture as a medium for CO_2 dissolution and ion transport [1]. Also, when the concrete is saturated fully, carbonation is very low due to the extremely slow diffusion of CO_2 through water-filled pores [11].

Material selection plays a critical role in determining the carbonation of concrete. The water to cement (w/c) ratio is one key factor: a lower w/c ratio leads to a denser microstructure with fewer capillary pores, resulting in a reduction of the permeability of CO_2 and increasing resistance to carbonation [12]. Additionally, the ratio of water to calcium oxide (CaO) in the binder affects the amount of $Ca(OH)_2$ available to react with CO_2. Gluth et. al. [13] demonstrated that concretes with lower water to CaO ratios exhibit slower carbonation due to the reduced availability of free water and a more compact matrix. The type of cement or SCM used can further affect how much $Ca(OH)_2$ is available to react.

Good curing, which requires adequate moisture retention of the cementitious material for complete hydration, is important too - especially for concretes with blended cements, because it helps form a denser surface that slows down CO_2 ingress [14].

The carbonation of concrete brings out both positive and negative effects on concrete. On the positive side, the compressive and tensile strengths of the unreinforced concrete can be enhanced by carbonation because the deposition of calcium carbonate makes the material more dense and less porous, creating a stronger and more durable surface layer [1]. For certain concrete materials, such as Ordinary Portland Cement (CEM I) concrete, carbonation has been shown to enhance mechanical properties, with moderate increases in compressive strength and elastic modulus under both ambient and elevated temperature conditions [15].

Carbonation is also of value from an environmental perspective as it makes concrete capable of capturing a considerable amount of the CO_2 emissions released when producing cement with the potential of compensating up to 75% of the limestone calcinations throughout the lifecycle of the material [16].

However, carbonation has shown more detrimental effects than the above-mentioned positive outcomes. The reduced alkalinity makes the steel susceptible to corrosion, which can lead to cracking, spalling, and ultimately a reduction in the durability and structural integrity of the concrete. The negative impact is especially pronounced in concrete with SCMs, such as fly ash, where carbonation can increase porosity and decrease both strength and stiffness. Thus, while carbonation can enhance certain properties of plain concrete, it poses a significant risk to the longevity of reinforced concrete structures if not properly managed.

1.1.3. Influence of Capillary Absorption and Compressive Strength on the Carbonation Resistance of Concrete

When evaluating the carbonation resistance of concrete, it is relevant to consider capillary absorption as an influencing indicator. This is because both transport processes (Carbonation and capillary absorption) are influenced by similar pore structure characteristics such as porosity and connectivity. CO_2 ingress occurs primarily through diffusion in the gas phase where the above characteristics play a key role [3,17]. Consequently, measuring capillary absorption provides practical insight into the transport network that also governs carbonation, helping us interpret and compare carbonation behavior more effectively.

Capillary absorption refers to the movement of water through the small pores in concrete without the influence of external pressure. This phenomenon is driven by surface tension forces and interactions between the water and the pore walls [18]. As discussed in Section 1.1.2, the porosity and permeability of concrete influence its carbonation rate. It has also been demonstrated that higher w/c ratios lead to increased initial absorption [17], as the pore structure becomes coarser and the total pore volume increases. Conversely, a lower w/c ratio results in a denser microstructure with finer pores, reducing permeability.

Furthermore, it has also been found that there exists a strong correlation between initial absorption, carbonation depth, and compressive strength at 28 days [17]. Specifically, lower initial absorption was associated with higher compressive strength and reduced carbonation depth, while higher initial absorption led to lower strength and deeper carbonation. The relationship between initial absorption and both compressive strength and carbonation depth was observed to be approximately linear.

1.1.4. Carbonation Resistance of Cementitious Systems with SCMs

The type and composition of SCMs significantly influence the carbonation resistance of concrete. Carbonation primarily affects the calcium-bearing phases in hydrated cement, especially $Ca(OH)_2$ and C-S-H. The carbonation rate of C-S-H is affected by its calcium to silicon (Ca/Si) ratio, with a lower Ca/Si ratio generally leading to increased carbonation [19].

Natural pozzolans, commonly used SCMs, are aluminosilicate materials, often of volcanic origin, that exhibit cementitious properties due to their high amount of reactive silica (SiO_2) and alumina (Al_2O_3) content [20]. Their incorporation typically reduces the Ca/Si ratio through pozzolanic reactions, forming secondary C-S-H from $Ca(OH)_2$ and contributing to a denser microstructure [19,21]. However, this may also reduce the amount of free $Ca(OH)_2$ available for carbonation, thereby dropping the pH even faster and decreasing carbonation resistance.

Curing plays a vital role when using pozzolanic SCMs. Insufficient curing increases permeability and reduces carbonation resistance, especially during early stages of hydration [14]. This highlights the need for extended curing when SCMs are used to ensure proper microstructural development.

Replacing Portland cement with SCMs also alters the pore structure and phase assemblage of the concrete, which can increase carbonation susceptibility [19]. Hence, finding solutions to mitigate this drawback is essential for ensuring long-term durability.

One such alternative SCM is iron silicate (IS), a pozzolanic byproduct of copper smelting, also referred to as copper slag. It contains oxides such as SiO_2, Al_2O_3, and CaO, which react with $Ca(OH)_2$ to form additional C-S-H, enhancing strength and durability [22–24]. Studies have shown that concrete incorporating IS can offer favorable mechanical performance and may reduce carbonation rates under certain conditions [23].

In a comparative study by Kaid et. al. [25], concretes with varying levels of natural pozzolans (70 kg/m³ and 105 kg/m³) exhibited higher carbonation depths than reference concrete with only Portland cement. Despite this, the mix with the highest pozzolan content also demonstrated superior compressive strength, highlighting the complex interactions between durability and mechanical properties.

1.2. Aim

One of the key challenges associated with using SCMs is their tendency to reduce early-age strength. To address this issue, several studies have investigated the potential of SEAs to enhance the early strength of concrete. In contrast, the application of SEAs in conjunction with pozzolans and slag has received significantly less attention, leaving a gap in research regarding their combined effect on mechanical properties and durability.

The aim of this master's thesis is to evaluate the influence of SEAs on the carbonation resistance, long-term strength development and capillary absorption of concrete incorporating selected SCMs and SEAs. However, as an initiative to the main aim, an analysis will be carried out to check the relationship between carbonation with capillary absorption and later age compressive strength.

The SCMs in focus are:
1. Volcanic Pozzolana Iceland (VPI)
2. Iron Silicates (IS)

VPI is mixed with the BAS cement powder which is included by the manufacturer Heidelberg Materials whereas IS is added separately to Akmenes Rapid Cement in the concrete mix design process. Further details about the SCMs are given in chapters 2.1.1 and 2.1.2

The SEAs used and tested in this experiment are,
1. Master X-Seed STE53
2. Master X-Seed 100

Both admixtures are tested in varying dosages within the selected SCM-containing cementitious systems. This research aims to assess their potential to improve concrete durability, with a focus on carbonation resistance, as well as mechanical performance in terms of later-age strength. These key aspects are evaluated under controlled experimental conditions.

1.3. Limitations

Due to time constraints and availability of materials, the scope of the study had to be limited. To be able to keep the number of concrete mixes being prepared at reasonable level, only concretes with commonly used water/binder (w/b) ratios (0,4, 0,5, 0,6) were prepared. 30 concrete mixes were initially proposed, but this number was reduced to 24 to make the workload manageable.

Since BAS VPI is a commercial product where VPI is one of the constituents, there was no possibility to prepare concrete mixes with only cement (without VPI) for result comparisons.

2. Materials

2.1. Cements

For the preparation of the concrete mixes, two different types of cement have been chosen to be able to get a better understanding of how strength enhancing admixtures affect concrete properties. The chosen cements are BAS VPI (CEM II) and Akmenes (CEM I). BAS VPI cement already has SCM, Volcanic Pozzolan Iceland, incorporated. Akmenes is pure cement, and the SCM, iron silicates, are added separately.

2.1.1. BAS VPI

Bascement Plus (BAS VPI) is a Portland composite cement, classified as CEM II/B-M (P-LL) with strength class 42,5R , and is produced in Slite. This cement incorporates natural pozzolan, Specifically Volcanic Pozzolan Iceland (VPI) a material with cement-like reactive properties, allowing it to partially replace traditional cement in the final mix. A key benefit of VPI is its minimal environmental impact in contrast to limestone, the primary raw material in cement production, which releases CO_2 during processing in cement kilns. By integrating VPI into the cement, the product achieves a notable reduction in CO_2 emissions.

Volcanic pozzolana, a natural SCM rich in amorphous silica and alumina, reacts with $Ca(OH)_2$ to form additional C-S-H gel. While this pozzolanic reaction can change the pore structure and improve the long term strength of concrete, it simultaneously reduces the free $Ca(OH)_2$ content, potentially accelerating carbonation under CO_2 exposure [26].

Table 2-1 shows the main constituents in the chemical composition of BAS VPI as reported by Heidelberg materials [27].

Table 2-1 Constituents of BAS VPI

Constituents	Percentage [wt %]
Portland cement clinker	≥68
Pozzolan + limestone	≤32

In the case of this study, the amount of VPI (pozzolan + limestone) is 30%, and subsequently the amount of Portland cement clinker is 70%.

Heidelberg materials report that the compressive strength of BAS VPI after 28 days of curing is 53 ± 4 MPa, which fulfills the requirements in the standard SS-EN 197-1:2011 for the strength class 42,5 R.

2.1.2. Akmenes Cement (CEM I 52,5R) and Iron Silicate

Akmenes Cementas is a Lithuanian cement manufacturer which produces cement according to the European Framework SS-EN 197-1:2011. The standard defines the requirements of what constituents are used in the cement and what mechanical, physical and chemical properties the cement requires.

The selected cement is Akmenes CEM I 52,5R. Akmenes Cemantas reports that the cement provides a compressive strength of ≥52,5 MPa after 28 days, which fulfills the standard SS-EN 197-1:2011 for the strength class 52,5 R.

As the cement is a CEM I it consists purely out of Portland cement clinker, except for a small percentage (0,1-5%) residual products from the production of cement clinker in the form of flue dust [28].

2.2. Coarse Aggregate

The coarse aggregate utilized in the concrete mixes for this study was provided by Skanska Industrial Solutions AB, specifically sourced from the Vikan quarry. A detailed petrographic analysis was conducted following RILEM AAR1.1:2016 guidelines, equivalent to the SS-EN 932-3:2022 standard, with additional quantitative thin-section microscopy analysis tailored for concrete applications.

Petrographic evaluation revealed the following predominant rock types:

- Paragneiss (approx. 75%), fine-to-medium-grained, biotite-rich with migmatitic sections containing coarse-grained feldspar and quartz.
- Granitic gneiss (approx. 14%), characterized by fine-to-medium grain size, containing feldspar, quartz, and biotite.
- Granodiorite (approx. 6%), granitoid in composition, typically massive to clearly foliated, containing feldspar, quartz, and biotite.
- Quartz fragments (approx. 5%) primarily derived from pegmatitic or migmatitic veins.

Quantitative mineralogical assessment indicated the dominant minerals in the coarse aggregate, which can be seen in Table 2-2. The presence of potentially alkali-silica reactive (ASR) minerals, specifically microcrystalline quartz, was limited to approximately 1% of the aggregate material, categorized as medium-to-slow reacting (Class II).

Table 2-2 Mineral constituents of coarse aggregate

Mineral	Percentage [vol %]
Quartz	34,6
Plagioclase	32,1
Potassium Feldspar	11,5
Biotite	10,6
Epidote	6,2
Muscovite	2,2

2.3. Fine Aggregate

The sand used in this study was supplied by Eurosand Export AB, sourced from the Arendal site. A comprehensive petrographic analysis has been carried out in accordance with SS-EN 932-3 and RILEM AAR1 standards, involving both microscopic examination and quantitative point-counting of mineral constituents.

The sand comprised entirely natural gravel (NG), characterized by rounded to irregularly shaped rock fragments and free mineral grains. Petrographically, the aggregate consisted predominantly of granitoids, quartz, and feldspar, constituting approximately 74 vol% of the fine fraction (0-2 mm) and 53% of the coarser fraction (2+ mm). Other significant constituents included quartzite, sandstone, fine-grained metabasalt/diabase, and volcanic rock fragments which can be seen in Table 2-3 below.

Table 2-3 Fine Aggregate Mineral Composition

Included aggregate/mineral	Vol % (0–2 mm)	Vol % (2+ mm A+B)
Granitoids, quartz, feldspar	73,6	53,0
Potentially reactive quartz, quartzite (ASR)	10,2	9,3
Siltstone, metasediment (ASR)	2,5	—
Quartzite, sandstone	5,1	6,2
Layered minerals (ASR)	0,3	0,7
Volcanite/mylonite/cataclasite (ASR)	0,9	1,3
Flint/chert (ASR)	3,0	8,5
Metabasite/diabase	3,5	9,3
Opaque (possibly sulfides, see below)	0,4	0,3
Free mica	—	0,6
Limestone/fossil (ASR)	—	3,5
Accessory grains	0,3	+
Total counted grains	1009 pcs. (One sample)	1134 pcs. (Two samples)

2.4. SCMs

2.4.1. Volcanic Pozzalana Iceland (VPI)

Table 2-4, which is an XRF provided by Thomas Concrete, shows the constituents of the chemical composition of VPI. As can be seen in the table, almost half of the material consists of silica dioxide (SiO_2), and the other half of the chemical composition mainly consists of aluminum oxide (Al_2O_3), iron(III) oxide (Fe_2O_3), calcium oxide (CaO) and magnesium oxide (MgO).

Table 2-4 Chemical Composition of VPI

Constituents	Percentage [wt %]
SiO_2	47,80
Al_2O_3	13,75
Fe_2O_3	12,13
CaO	12,05
MgO	10,78
Na_2O	1,92
K_2O	0,34
Mn_2O_3	0,23
P_2O_5	0,19

2.4.2. Iron Silicates (IS)

The chemical composition of IS is shown in Table 2-5 below, which is an XRF provided by Thomas Concrete. The main constituents of the material are Fe_2O_3, SiO_2 and Al_2O_3

Table 2-5 Chemical Composition of Iron Silicate

Constituents	Percentage [wt %]	Constituents	Percentage [wt %]
Fe_2O_3	40,8	CuO	0,11
SiO_2	29,3	ZnO	0,10
Al_2O_3	8,65	SO_3	0,08
LOI	2,76	P_2O_5	0,05
MgO	2,63	NiO	0,03
CaO	2,55	V_2O_5	0,02
Cr_2O_3	0,59	MoO_3	0,02
MnO	0,37	CoO	0,01
K_2O	0,14	SrO	0,01
TiO_2	0,13	ZrO_2	0,01
Na_2O	0,12		

2.5. Strength Enhancers

Strength-enhancing admixtures (SEAs) are chemical additives developed to improve both the early-age and later-age mechanical performance of concrete. In this study, two SEAs were tested: Master X-Seed STE53 and Master X-Seed 100. These products utilize advanced seeding technology to accelerate the hydration process of cement particles by introducing synthetic C-S-H crystals of nano-size into the concrete mixture [29].

The cement hydration process begins with a reaction between cement clinker and water, involving a dissolution and recrystallization sequence that produces C-S-H gel. The introduction of C-S-H nanoparticles through SEAs accelerates the early stages of this reaction by providing nucleation sites for further C-S-H formation.

Nucleation is a process where clusters of a stable phase becomes less stable, and is the first step in a lot of phase transformations (for example solidification of liquids) [30]. In the case of cement, nucleation have a big effect on the microstructure of C-S-H gel and subsequently the pore size distribution of hardened cement paste [30]. This promotes faster strength development at early ages, particularly beneficial when using blends with high SCM-content [29].

Master X-Seed 100 is a suspension of C-S-H nanoparticles with an approximate solid content of 23 wt% [31]. In contrast, Master X-Seed STE53 is a similar product that contains both C-S-H nanoparticles and alkanol amides, with a higher solid content of approximately 28 wt% [32].

Both admixtures are formulated in a chemical suspension that includes superplasticizers and other auxiliary compounds. However, the specific types of superplasticizers or dispersing agents used in the suspension are not available in the product data sheets and literature due to company confidentiality.

The use of these admixtures can enable cement reductions while maintaining mechanical strength and durability performance, thus supporting more sustainable concrete mix designs and contributing to lower CO_2 emissions from cementitious materials [29,31,32].

3. Method

The methodology of this study consists of tests being performed on concrete specimens to evaluate the carbonation rate for the different cementitious systems containing SEAs and the properties it affects, compressive strength and capillary absorption. Before being able to perform the tests, it was needed to first understand the theory behind carbonation and capillary absorption and what parameters would affect the results of the tests. Then the mixing of the concrete specimens was done according to standards depending on what test the specimen was intended for, and finally the compressive strength, carbonation and capillary absorption tests were performed.

This chapter describes the theory behind carbonation and capillary absorption testing and result analysis first, then the mixing procedure for making concrete specimens, and finally the procedure for the performed tests and their followed standards.

The tests that were performed were compressive strength testing to evaluate the mechanical performance of the specimen and the carbonations influence (see chapter 3.3.1), accelerated carbonation testing (see chapter 3.3.2.), and capillary absorption testing to evaluate the carbonations influence on durability (see chapter 3.3.3.).

3.1. Theory

In the following subchapters 3.1.1. and 3.1.2., the equations that are used to calculate carbonation and capillary absorption and the parameters that affect the results are explained to gain a better understanding of the methodology of the tests.

3.1.1. Carbonation

As mentioned in Chapter 1.1.2, Carbonation is the process where CO_2 from the air moves into the concrete's pore system and reacts with hydration products. Measurement of carbonation of concrete can be carried out using several models and methods. However, for this study, the most common model based on Ficks first law has been preferred. This model proposed by Tuutti [12] is based on the diffusion law and considers that the carbonation rate is proportional to the square root of the time of exposure to the CO_2 [33].
Equation (2):

$$X(t) = k_{carb} * \sqrt{t} \qquad (2)$$

X(t) is the carbonation depth after a certain time of exposure to CO_2 [mm/year]

k_{carb} is the carbonation coefficient taking in consideration the environmental conditions and concrete quality [mm/year^{0,5}]

t is the time [years]

The carbonation coefficient k_{carb} is determined by plotting the measured carbonation depth against the square root of the exposure time. The value of k_{carb} is obtained from the slope (gradient) of the best-fit line through the plotted measurements. The resultant k_{carb} values can be seen in chapter 4.2 and Appendix B1.

As observed here, $\sqrt{t}$ is used instead of t for plotting. The reason for this is the assumption that carbonation is a diffusion-controlled process, and according to Fick's first law of diffusion, the depth of penetration of a diffusing substance (in this case, CO_2) is proportional to the square root of time [2,34]

A higher k_{carb} value indicates a faster rate of carbonation, which suggests lower resistance of the concrete to carbonation whereas a lower k_{carb} value indicates slower rate of carbonation.

3.1.2. Capillary Absorption

Capillary absorption refers to the "uptake of water into the pore structure of concrete due to capillary forces, driven by differences in vapor pressure within the material's porous network" according to NT Build 368,1991. This process is particularly important in assessing the durability of concrete, as water ingress can transport harmful substances such as chlorides and CO_2, accelerating degradation processes like corrosion and carbonation.

The rate of capillary absorption is commonly characterized by the capillary absorption coefficient, which quantifies the amount of water absorbed per unit area over time. According to the standardized procedure outlined in NT Build 368,1991 (refer to section 3.3.3), the capillary coefficient k_{cap} can be calculated using the following equation:

$$k_{cap} = \frac{Q_{cap}}{\sqrt{t_{cap}}} \left[\frac{kg}{m^2\sqrt{s}}\right] \quad (3)$$

Q_{cap} is the amount of absorbed water [kg/m^2]
t_{cap} is the time to complete the capillary absorption [s]

Since capillary absorption is also a diffusion-controlled process, $\sqrt{t_{cap}}$ is plotted instead of t. It is plotted against Q_{cap} which can be calculated using the weight and the dimensions of the sample.

The capillary coefficient k_{cap} quantifies how quickly water is drawn into a porous material through capillary action. A higher k_{cap} means water penetrates the material more rapidly and to greater depths over a given period.

For cross validation, reducing the area differences of specimen and directly getting resistance, the resistance number m_{cap} is also used for capillary absorption results analysis. The resistance number can be calculated using the following equation (4):

$$m_{cap} = \frac{t_{cap}}{h^2} \ (s/m^2) \quad (4)$$

m_{cap} = resistance coefficient (s/m^2)
t_{cap} = time to completion of capillary absorption (s)
h = thickness of the specimen (m)

Concrete with a more refined and disconnected pore system, typically achieved through lower w/b ratios, SCMs, or chemical admixtures, tends to exhibit lower capillary absorption rates [15]. Higher porosity as well as poor curing of concrete can cause considerably higher absorption, hence a lower durability as well as service life of the structure.

Capillary absorption monitoring is therefore a key consideration for durability design and mechanical properties improvement, particularly for building elements subjected to severe environmental conditions. In this study, a specific effort has been made to correlate the capillary absorption to carbonation of the selected cementitious mixes containing SCMs and SEAs.

3.2. Specimen preparation for testing

3.2.1. Mixing and Casting

The first step of the experimental work was to mix the different concrete binders that were to be used for the tests.

Concrete specimens with different types of cement, w/b ratios, and different SCMs and SEAs (Varying dosage of SEA in some cases) were prepared to get a better understanding of how the accelerators affect the concrete with regards to the mechanical properties and durability. Concrete specimens with no SEAs were also prepared to have reference specimens to compare the result of the SEAs to. Due to miscalculations when preparing the mixes, an additional BAS VPI mix with 0,2% Master X-Seed STE53 and w/b ratio 0,4 was prepared that was not included in the initial plan, but was kept for testing.

The full list of BAS VPI mixes can be found in Table 3-1 and Akmenes mixes in Table 3-2 below.

Table 3-1 List of BAS VPI Mixes

SCM	SCM Dosage [wt %]	w/b ratio	SEA	SEA Dosage [wt %]
VPI	30	0,4		
VPI	30	0,5		
VPI	30	0,6		
VPI	30	0,4	Master X-Seed STE53	2
VPI	30	0,5	Master X-Seed STE53	2
VPI	30	0,6	Master X-Seed STE53	2
VPI	30	0,4	Master X-Seed STE53	4
VPI	30	0,5	Master X-Seed STE53	4
VPI	30	0,6	Master X-Seed STE53	4
VPI	30	0,4	Master X-Seed 100	4
VPI	30	0,5	Master X-Seed 100	4
VPI	30	0,6	Master X-Seed 100	4
VPI	30	0,4	Master X-Seed STE53	0,2

Table 3-2 List of Akmenes Mixes. The last three mixes (denoted -----) are pure Akemens, i.e.,

SCM	SCM Dosage [wt %]	w/b ratio	SEA	SEA Dosage [wt %]
IS	25	0,4		
IS	25	0,5		
IS	25	0,6		
IS	25	0,4	Master X-Seed STE53	2
IS	25	0,5	Master X-Seed STE53	2
IS	25	0,6	Master X-Seed STE53	2
IS	25	0,4	Master X-Seed STE53	4
IS	25	0,5	Master X-Seed STE53	4
IS	25	0,6	Master X-Seed STE53	4
-----	0	0,4		
-----	0	0,5		
-----	0	0,6		

For the specimen preparation procedure for both compressive strength and carbonation, standard SS-EN 12390-2:2019 was followed.

After each binder was mixed, the mix was divided into different molds to prepare specimens of different shapes that fulfill the standards they were intended for. For the compressive strength and carbonation tests, the casting was done in steel molds which fulfill the standard SS-EN 196-1:2016. According to the standard, the mold should consist of 3 prismatic compartments with the size 40mm*40mm*160mm. For each mix, 6 specimens (2 molds) were casted to have 2 specimens per testing case for higher accuracy. A vibrating table was used for the compaction of the mixes, and afterwards the top surface of the specimen was leveled carefully to obtain concrete prisms with as even surfaces as possible.

Specimens for capillary absorption testing were prepared based on the methodology outlined in NT Build 368,1991, a standardized test method developed by NordTest for assessing concrete properties. The concrete mixes were poured into cylindrical molds in one layer. The top surface was leveled carefully after vibration, and the molds were then covered to prevent moisture loss during the initial setting period just as for the prisms.

There were specific modifications made to accommodate the available equipment and research scope. While NT Build 368,1991 recommends using cylindrical specimens of 100 mm diameter and 20 mm height, in this study, cylindrical specimens of 100 mm diameter and 140 mm height were cast. This deviation from the standard was necessary due to mold limitations and post-curing cutting requirements. As a result of the increased height, vibration was applied during casting to eliminate entrapped air and ensure adequate compaction, a notable difference from the NT Build recommendation, which suggests non-vibrated casting to preserve natural pore structure. Further deviations from the standard regarding the curing are explained in section 3.2.3.

3.2.2. Curing

After the specimen was cast, they were covered using polyethylene to prevent moisture loss. After approximately 24h, the polythene covers were removed, and the specimen were demolded. Then the specimen was appropriately labelled and submerged in water with a temperature of 20°C to cure in accordance with SS-EN 12390-2:2019 (except for the capillary absorption specimen which follow NT Build 368,1991), for different durations depending on the specific test requirements. The designated curing periods were as follows:

- Compressive strength testing: 28 and 56 days
- Carbonation testing: 28 days
- Capillary absorption: 56 days

After curing the top and bottom surface of the carbonation prisms were painted using epoxy to allow uni - directional carbonation. After that, the specimens were conditioned in laboratory air (20C, ~50% RH) for 14 days to allow for moisture equilibrium before being transferred to the carbonation chamber.

For capillary absorption, the standard NT Build 368,1991 states that the curing period should be 28 days, but given that most of the mixes contained SCMs - which are known to hydrate more slowly than OPC, the curing period was extended to 56 days. This allowed for more complete hydration and development of the pore structure, especially for pozzolanic materials.

At the end of the 56-day curing period, the cylindrical specimens were precisely cut to a height of 20 mm using a diamond saw to match the dimensions specified in NT Build 368,1991. These cut sections were then used for the capillary absorption test, following the subsequent surface preparation and sealing procedures outlined in the standard.

3.3. Testing

The experimental methodology followed established European and Nordic testing standards. Compressive strength testing was conducted according to SS-EN 196-1:2016, which specifies procedures for preparing and testing cement mortar prisms under controlled conditions to assess strength development. Carbonation resistance was evaluated in line with SS-EN 12390-12:2020, a standard that outlines accelerated testing of carbonation depth in hardened concrete using controlled CO_2 exposure. For capillary absorption, NT Build 368,1991 was used as mentioned in 3.2.1, which describes a method to measure the water absorption of concrete through capillary action under standardized conditions.

3.3.1. Compressive Strength

The standard SS-EN 196-1:2016 states that for compressive strength testing, the specimens should be loaded with rate of load increase of 2400 ± 200 N/s. The force of the load should pass through the center of the specimens and be applied until failure. To fulfill these requirements, a Form+Test Seidner CSRG-5503 compression testing machine was used, shown in Figure 3-1. The machine was able to provide the load rate of 2400 N/s required.

Figure 3-1 Compressive Strength Testing Form+Test Seidner CSRG - 5503

For the testing, 4 concrete prisms were tested from each concrete mix to be able to give a mean value of the compressive strength for each concrete mix according to SS-EN 196-1:2016. Results that differed by more than ±10% from the mean of the other results for prisms of the same mix were discarded to get a more reliable mean value.

When the compressive strength testing was performed, the prisms were loaded at the center of the longitudinal direction. The load was applied downwards until the prisms reached failure. The tests were performed after 28 days to determine the strength of the concrete mixes and after 56 days to evaluate the increase in compressive strength after extended curing. The results were given in kN, while the standard SS-EN 196-1:2016 states that results should be given in MPa with an accuracy of 0,1 MPa. Therefore, the results was divided by a factor of 1,6 for conversion.

3.3.2. Carbonation

The carbonation resistance of concrete was evaluated using an accelerated carbonation test method based on SS-EN 12390-12:2020. According to the standard, after the concrete specimens have been casted and cured for 28 days, they were placed in a storage chamber and exposed to a CO_2 concentration of 3 ± 0,5% at a temperature of 20 ± 2°C and a relative humidity of 57 ± 3% for up to 70 days. This is to expose the concrete specimens to a controlled CO_2 environment to be able to measure the carbonation depth earlier than for natural carbonation. The recommended periods for exposure in the storage chamber are 7, 28 and 70 days. After each period, a slice of approximately 50 mm of a specimen should be broken off and the rest of it should be put back in the chamber. To measure the carbonation depth, the standard states that a suitable indicator that gives a color change in pH range of 8 to 11 should be applied, and 12 points of carbonation depth should be measured, out of which the mean value is taken.

Specimens were exposed in this chamber for up to 56 days and carbonation depth was to be assessed at 5 pre-planned time intervals: 0, 14, 28, 42 and 56 days. However, due to technical difficulties, the results were instead taken on 29, 40 and 54 days. Since the aim is to find the

rate of carbonation and the number of results does not change, this slight difference in testing days provides a negligible difference.

At each testing age, a ~30mm part was removed from the specimen using the compressive strength testing machine. To determine the carbonation depth in the concrete specimens the pH indicator thymolphthalein was sprayed on the freshly broken surfaces both on the remaining large part and the broken off part to indicate the carbonation front. Thymolphthalein results in a color change when the pH-value of a surface is somewhere in the range of 9,3 to 10,5, and when applied to concrete it has a blue color when the pH of the concrete is higher and is colorless when it's lower and carbonation is present [35].

The pore solution of concrete usually have a pH-value of around 12,5-13,9 [36]. In the case of carbonation, the pH-value drops to levels of neutrality.

After applying the indicator, six points were measured on the remaining specimen and six points on the broken part. The direction in which the measurements were taken can be seen in figure 3-2. The average of these measurements was taken for each specimen, and the mean of the two specimens at each exposure time was reported as the carbonation depth for that period.

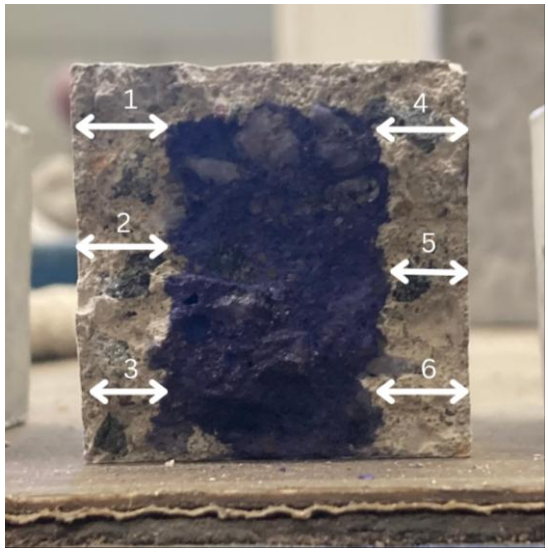

Figure 3-2 Six Measurements per face for carbonation depth

After the tests were performed, the carbonation coefficients k_{carb} were obtained according to equation (2).

3.3.3. Capillary Absorption

After the completion of the mixing and curing procedures mentioned in sections 3.2.1 and 3.2.3 respectively, the capillary absorption test was performed. Specimens were placed upright in a vessel and covered from the top to minimize evaporation as seen in Figure 3-3. To ensure unidirectional water absorption, the bottom surface was placed in contact with wet wettex cloth. Mass measurements were taken at standard time intervals as outlined in NT Build 368,1991.

Figure 3-3 Capillary Absorption Specimen Setup

The standard time points of 10 minutes, 30 minutes, 1 hour, 2 hours, 4 hours, and 6 hours could only be followed for specimens with a w/b ratio of 0,4. For the 0,5 and 0,6 w/b ratio specimens, the 6-hour measurement was replaced with a 5-hour reading. Measurements continued on Day 2 through Day 7 to track longer-term water uptake which is a result of diffusion.

As per NT Build 368,1991, specimens should be saturated by submersion in water for 3 days, followed by pressurized saturation at 80 atmospheres for another 3 days. However, since the 0,6 w/b ratio specimens appeared fully saturated after the 7-day capillary absorption and diffusion, the pressurized saturation step was omitted for these samples. For the 0,4 and 0,5 w/b ratio specimens, the full saturation procedure was completed.

Finally, all specimens underwent vacuum saturation, a process in which the concrete samples are placed in a sealed chamber and subjected to a vacuum to remove air from the pore structure. Once the air is evacuated, water is introduced into the chamber, allowing it to be drawn into the pores under the vacuum pressure. This ensures that the internal pore volume is fully saturated with water, which enables us to calculate total porosity which is a necessary capillary absorption parameter. This step was followed by submersion in water for 10 hours. The final step involved oven drying at 105°C until a constant mass was achieved, after which the dry weights were recorded. This step is essential to calculate both active and total porosity. Equations for active porosity can be found in section 4.3.3.

To be able to obtain the capillary coefficient k_{cap} and the resistance number m_{cap} from the measurements, the water absorption is plotted against the square root of time. As is shown in NT Build 368,1991 and in sample Figure 3-4, the plotted absorption curve can be simplified in two different regression lines. The first regression line is the water absorption due to capillary absorption and the second is the water absorption due to diffusion. However, there is no standard to pinpoint the exact time capillary absorption stops and diffusion starts.

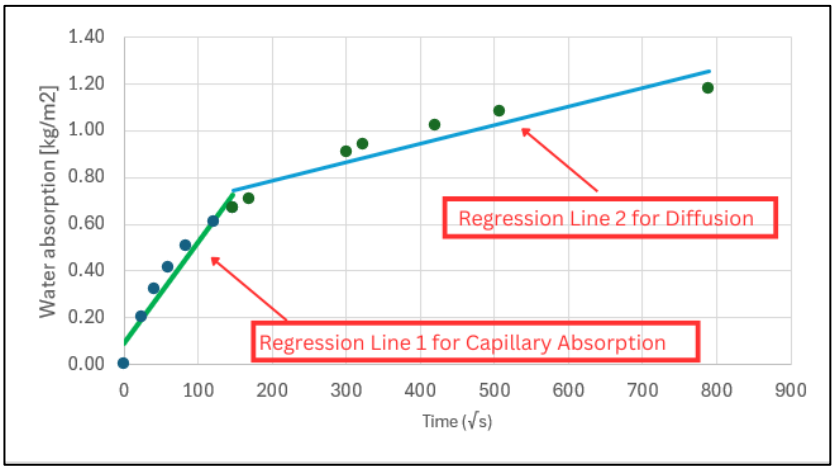

Figure 3-4 Regression Lines (Example) for Capillary Absorption and Diffusion

Therefore, ASTM standard (C1585) has been used as a reference which states, "For the regression analysis, use all the points from 1 min to 6 h, excluding points for times after the plot shows a clear change of slope. If the data between 1 min and 6 h do not follow a linear relationship (a correlation coefficient of less than 0.98) and show a systematic curvature, the initial rate of absorption cannot be determined."

Using this as a foundation, the regression lines have been drawn
1. from 1min to 6h
2. from 6h onwards

The regression lines have been built using the standard linear equation showed in equation (5).

The regression line $y = ax + b$ *(5)*

a – slope of the equation
b – intercept of the y axis

These two variables can be found using the following equations (6) and (7).

$$a = \frac{n\sum xy - \sum x \sum y}{n\sum x^2 - (\sum x)^2} \quad (6)$$

$$b = \frac{\sum y - a\sum x}{n} \quad (7)$$

n = *number of data points* $\sqrt{t}$
$\sum x$ = *sum of all* x *values*
$\sum y$ = *sum of all* y *values*
$\sum xy$ = *sum of the products* $x \times y$ *for each data pair*
$\sum x^2$ = *sum of the squares of the* x *values*

4. Results

4.1. Compressive Strength

4.1.1. Compressive strength for w/b ratio 0,4

Figure 4-1 shows the compressive strength result for the BAS VPI mixes with a w/b ratio of 0,4. As can be seen in the figure, the highest compressive strength after 28 days was measured for the mix containing 2% of Master X-Seed STE53, with a mean compressive strength of 76,4 MPa. The lowest mean compressive strength after 28 days was measured for the mix with no SEA, being 72,0 MPa.

For the 56 days compressive strength testing, the highest mean compressive strength was measured for the mix containing 0,2% of Master X-Seed STE53 with a mean compressive strength of 83,1 MPa. The lowest mean compressive strength was measured for the BAS VPI with no SEA, with a value of 63,9 MPa.

The biggest increase in mean compressive strength between the two tests was seen for the mix with 0,2% Master X-Seed STE53, which increased by 8,52 MPa. For the mixes with no SEA and 2% Master X-Seed STE53, the mean compressive strength decreased significantly between the 28 days and 56 days tests due to outliers in the testing. Outliers were specimen with compressive strength results that deviated more than ±10% from the mean result of the other specimens in the same mix, in accordance with SS-EN 196-1:2011 as stated in section 3.3.1. These outliers were removed to get more reliable results, but there was still a noticeable decrease in mean compressive strength. The mix with no SEA decreased by 8,1 MPa, while the mix with 2% Master X-Seed STE53 decreased by 3,2 MPa. The lowest strength increase aside from the faulty concretes was the BAS VPI concrete with 4% Master X-Seed 100 which increased 2,8 MPa, from 75,9 MPa to 78,7 MPa.

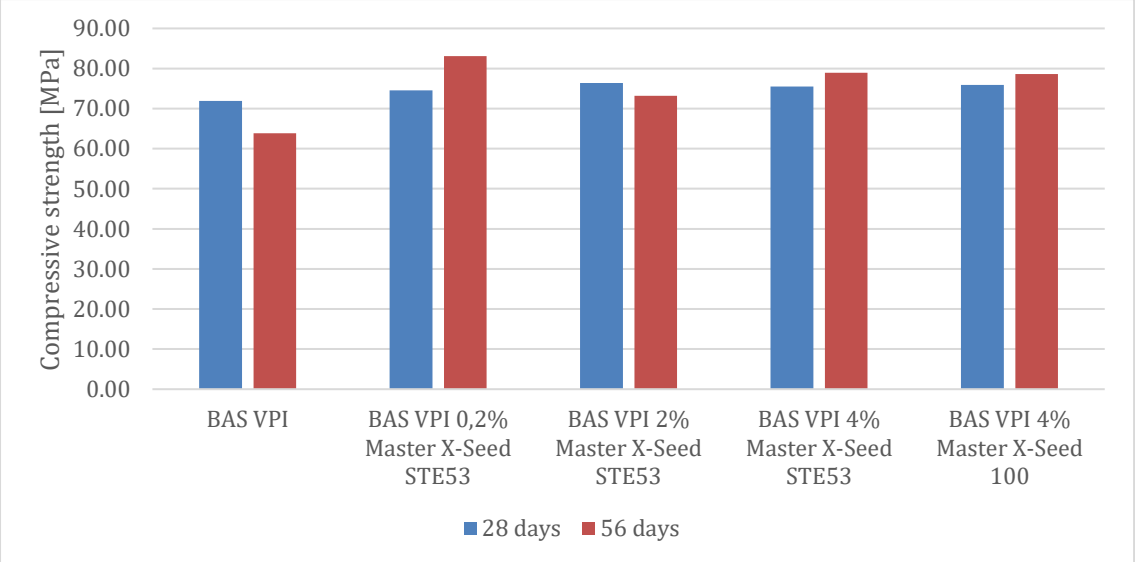

Figure 4-1 Results for compressive strength tests for BAS VPI mixes with w/b 0,4. The values for compressive strength is given in Appendix A1 (in Appendix A3, the mixes with decreasing strength results with and without outliers are shown)

Figure 4-2 shows the compressive strength results for Akmenes mixes with w/b ratio of 0,4.

The highest mean compressive strength for 28 days testing was measured for the mix with 25% IS and 2% Master X-Seed STE53, being 64,3 MPa. The lowest compressive strength was measured for the mix containing 25% IS and no SEA, with a mean compressive strength of 57,6 MPa.

The 56 days strength testing results shows that the mix with 25% IS and 2% Master X-Seed STE53 still have the highest mean compressive strength of 71,8 MPa. The mix with 25% IS and no SEA still have the lowest mean compressive strength of 60,6 MPa.

The biggest improvement in strength between the two tests was seen for the mix with 4% Master X-Seed STE53 which increased 8,8 MPa. The smallest improvement in compressive strength was seen for the mix only containing 25% IS, which increased 3,0 MPa in strength.

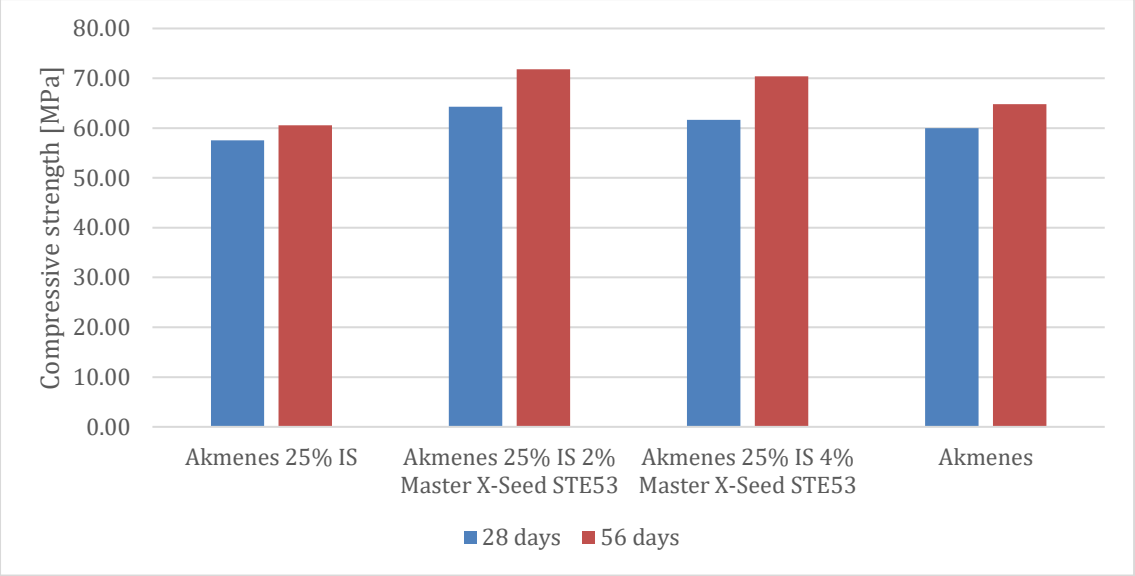

Figure 4-2 Results for compressive strength tests for Akmenes mixes with w/b 0,4. The compressive strength values are shown in Appendix A2.

4.1.2. Compressive strength for w/b ratio 0,5

Figure 4-3 shows the mean compressive strength results for all BAS VPI mixes with a w/b ratio of 0,5. It can be seen that the highest mean compressive strength after 28 days was measured for the mix with 4% Master X-Seed 100, with a mean compressive strength of 60,7 MPa. The lowest mean compressive strength after 28 days was measured for the mix with no SEA, with a mean compressive strength of 53,2 MPa.

The highest mean compressive strength after 56 days was measured for the mix with 4% Master X-Seed STE53, with a mean compressive strength of 65,6 MPa. The lowest mean compressive strength after 56 days was measured for the mix with no SEA, being 54,1 MPa.

The biggest increase in compressive strength was seen for the mix with 4% Master X-Seed STE53, as it increased 4,9 MPa in strength. The lowest increase was measured for the mix with no SEA, which only increased 0,8 MPa in compressive strength.

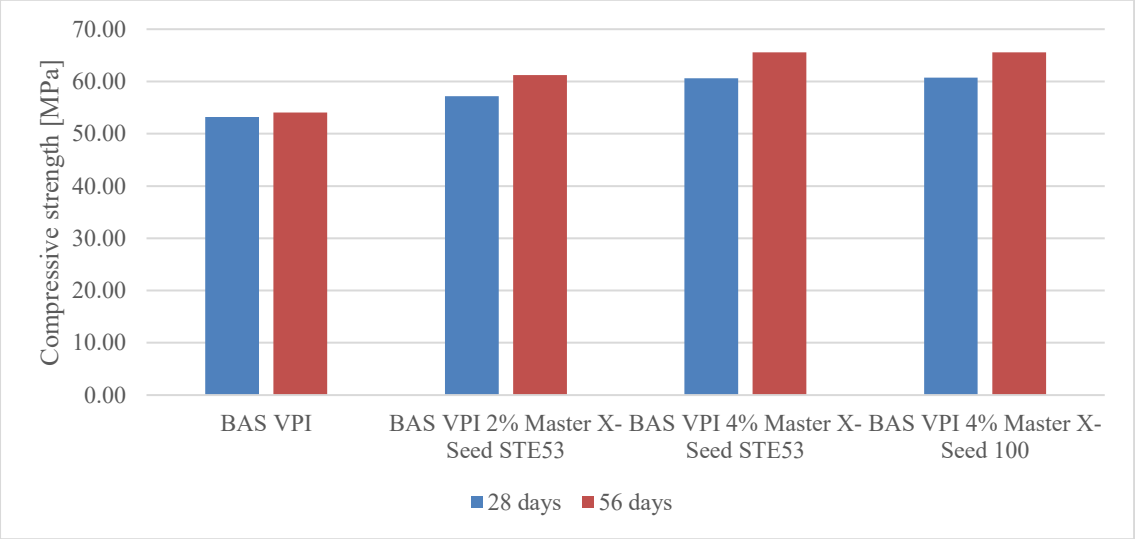

Figure 4-3 Results for compressive strength tests for BAS VPI mixes with w/b 0,5. The compressive strength values are shown in Appendix A1.

Figure 4-4 shows the compressive strength results for Akmenes mixes with a w/b ratio of 0,5. The highest mean compressive strength after 28 days was measured for the mix with only Akmenes cement, being 50,5 MPa. The lowest mean compressive strength was measured for the mix with 25% IS and no SEA, being 42,4 MPa.

The highest mean compressive strength after 56 days was measured for the mix with 4% Master X-Seed STE53, being 53,2 MPa. The lowest strength was once again measured for the mix with only 25% IS and no SEA, being 47,2 MPa.

The biggest improvement in compressive strength was seen for the mix with 4% Master X-Seed STE53, with an increase in strength of 5,2 MPa. The lowest increase was seen for the mix with no IS or SEA, only increasing by 1,1 MPa.

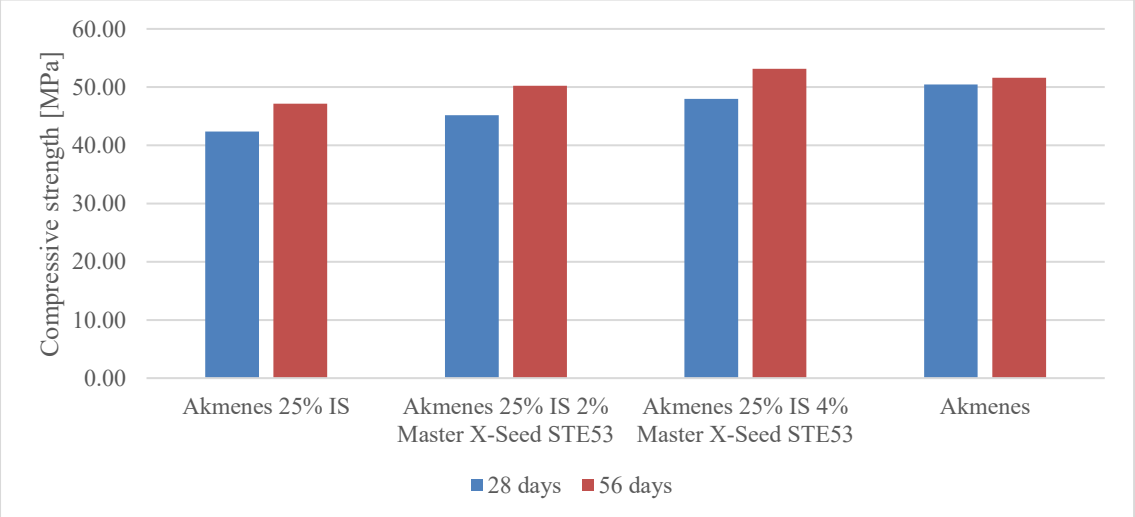

Figure 4-4 Results for compressive strength tests for Akmenes mixes with w/b 0,5. The compressive strength values are shown in Appendix A2.

4.1.3. Compressive strength for w/b ratio 0,6

Figure 4-5 shows the mean compressive strength results for all BAS VPI mixes with a w/b ratio of 0,6. The highest mean compressive strength after 28 days was measured for the mix with 4% Master X-Seed STE53, with a mean compressive strength of 46,2 MPa. The lowest mean compressive strength was measured for the mix with no SEA, being 37,9 MPa.

The highest mean compressive strength after 56 days was measured for the mix with 4% Master X-Seed STE53, with a mean compressive strength of 52,0 MPa. The lowest strength was measured for the mix with 2% Master X-Seed STE53, being 42,0 MPa.

The biggest increase in mean compressive strength was measured for the mix with no SEA, which increased by 8,5 MPa in compressive strength

For the mix with 2% Master X-Seed STE53, the compressive strength decreased by 2,1 MPa, and the smallest increase in strength was seen for the mix with 4% Master X-Seed 100 being 4,5 MPa.

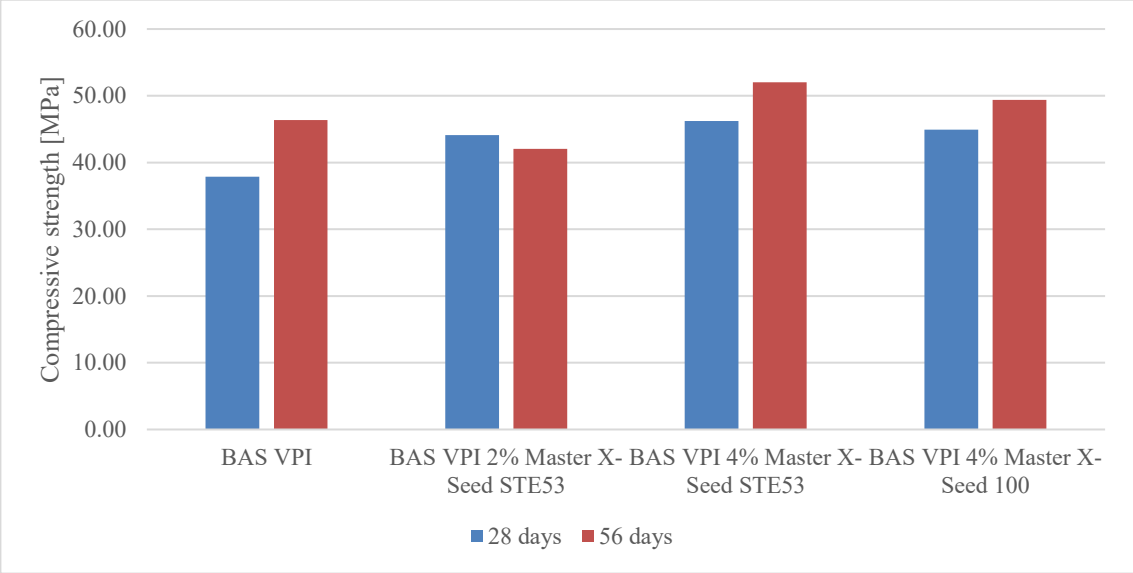

Figure 4-5 Results for compressive strength tests for BAS VPI mixes with w/b 0,6. The compressive strength values are shown in Appendix A1.

Figure 4-6 show the mean compressive strength for all Akmenes mixes with w/b ratio 0,6. It can be seen that the highest mean compressive strength after 28 days was measured for the mix with no IS or SEA, with a value of 40,7 MPa. The lowest mean compressive strength was measured for the mix with 25% IS and no SEA, being 28,1 MPa

For 56 days compressive strength testing, the highest mean compressive strength was once again seen in the mix with no IS or SEA, with a value of 42,6 MPa. The mix with the lowest mean compressive strength was the one with 25% IS and no SEA, having a strength of 32,9 MPa.

The biggest increase in mean compressive strength was measured for the mix with 4% Master X-Seed STE53, being 4,9 MPa. The lowest increase was measured for the mix with no IS or SEA, which had an increase of only 1,9 MPa.

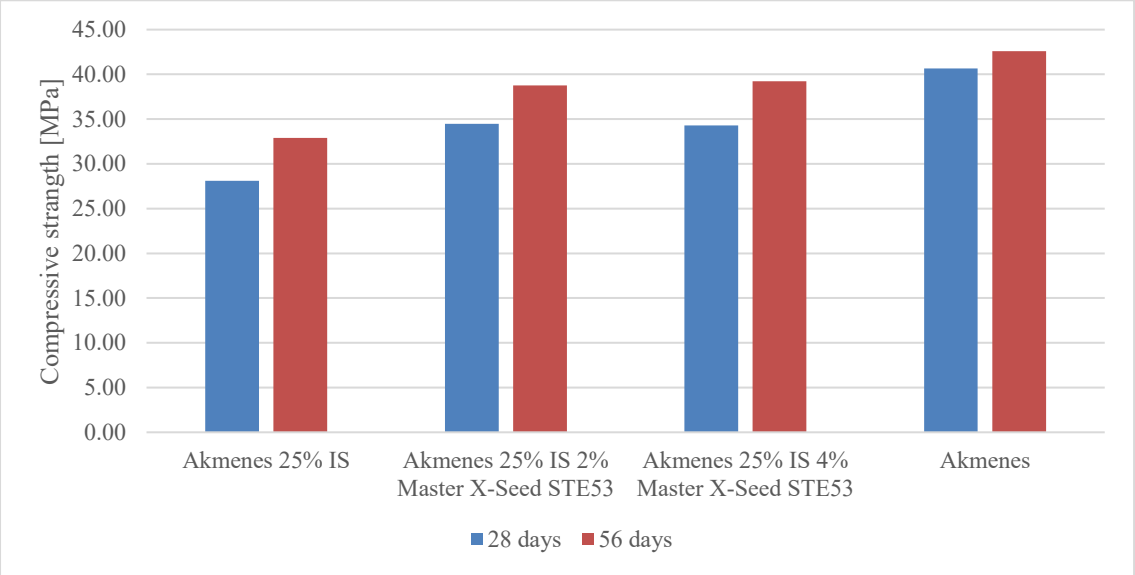

Figure 4-6 Results for compressive strength tests for Akmenes mixes with w/b 0,6. The compressive strength values are shown in Appendix A2.

The results in sections 4.1.1. to 4.1.3. show that BAS VPI mixes generally exhibits higher mean compressive strengths (in the range of 37,9 MPa to 76,4 MPa for 28 days and 42,0 MPa to 83,1 MPa for 56 days) than Akmenes mixes (in the range of 28,1 MPa to 64,3 MPa for 28 days and 32,9 MPa to 71,8 MPa for 56 days), and that the inclusion of SEAs leads to an increase in strength. The increase in strength between 28 days and 56 days of curing were also generally higher when including SEAs.

4.2. Carbonation

Figure 4-7 shows carbonation coefficients k_{carb} describing carbonation rates for the BAS VPI mixes, and the highest values are measured for mixes with a w/b ratio of 0,6 in the range of 1,86 mm/√days to 2,25 mm/√days. k_{carb} become lower when the w/b ratio is lowered, with the mixes with a ratio of 0,5 having values between 1,12 mm/√days and 1,31 mm/√days. For w/b ratio 0,4 k_{carb} were low, ranging between 0,51 mm/√days and 0,73 mm/√days. The highest k_{carb} was measured for BAS VPI with no SEA and a w/b ratio of 0,6, being 2,25 mm/√days. The lowest k_{carb} was measured for the mix with 0,2% Master X-Seed STE53, being 0,51 mm/√days.

Mixes containing Master X-Seed STE53 showed lower k_{carb} values compared to the mixes with no SEA. For 2% Master X-Seed STE53 the value decreased by 0,05 mm/√days for w/b ratio 0,4, 0,07 mm/√days for w/b ratio 0,5 and 0,32 mm/√days for w/b ratio 0,6.

4% of Master X-Seed STE53 showed greater improvements, decreasing k_{carb} by 0,11 mm/√days for w/b ratio 0,4, 0,19 mm/√days for w/b ratio 0,5 and 0,39 mm/√days for w/b ratio 0,6.

The positive effect of Master X-Seed 100 was somewhat inconsistent, as k_{carb} increased by 0,05 mm/√days for w/b ratio 0,4, but decreased by 0,18 mm/√days for w/b ratio 0,5 and 0,21 mm/√days for w/b ratio 0,6.

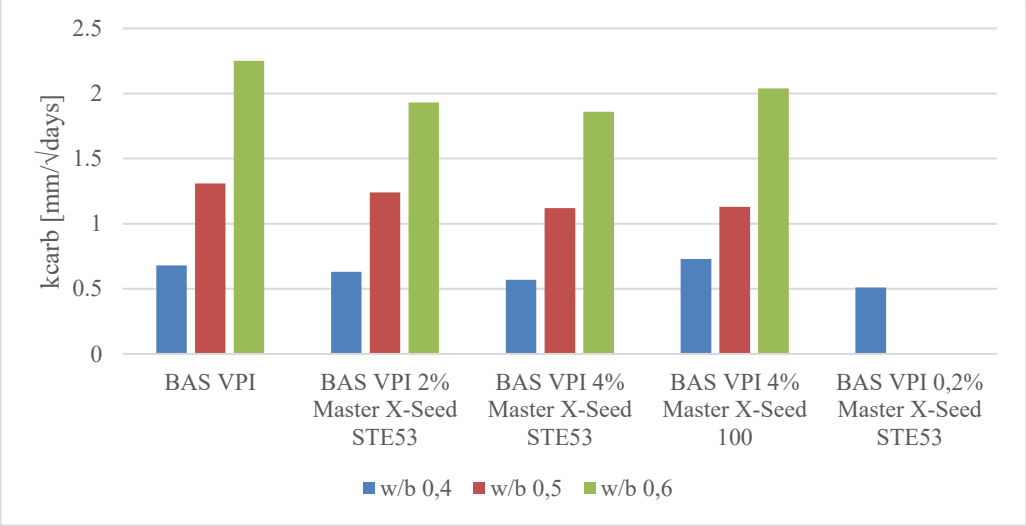

Figure 4-7 Carbonation coefficients k_{carb} for BAS VPI mixes. All values for k_{carb} is shown in Appendix B1.

Figure 4-8 shows k_{carb} for all Akmenes mixes. The results follow the same pattern as for the BAS VPI mixes, with higher k_{carb} for high w/b ratios. For mixes with a ratio of 0,6 k_{carb} ranges between 1,74 mm/√days and 2,85 mm/√days. For w/b ratio 0,5 k_{carb} is significantly lower ranging between 0,89 mm/√days and 2,3 mm/√days. The rates decrease even more for w/b ratio 0,4, with k_{carb} ranging between 0,26 mm/√days and 0,96 mm/√days. The highest k_{carb} that was measured for Akmenes mixes was found in the mix with 25% IS and 2% Master X-Seed STE53, w/b ratio 0,6, which was 2,85 mm/√days. The lowest k_{carb} was found in the mix with no IS or SEA, w/b ratio 0,4, which was as low as 0,26 mm/√days.

Mixes containing Master X-Seed STE53 mostly showed an improvement in k_{carb} values compared to the mixes with no SEAs. In the case of 2% Master X-Seed STE53, k_{carb} decrease 0,16 mm/√days for w/b 0,4 and 0,53 mm/√days for w/b 0,5. For w/b 0,6 k_{carb} increase slightly by 0,03 mm/√days.

4% of Master X-Seed STE53 gives a more consistent improvement, decreasing the k_{carb} for all w/b ratios. k_{carb} is decreased by 0,23 mm/√days for w/b ratio 0,4, for ratio 0,5 it decreases by 0,74 mm/√days, and 0,18 mm/√days for ratio 0,6.

Pure Akmenes mixes with no IS or SEA exhibited the lowest k_{carb} by a large margin out of all mixes for each w/b ratio. The k_{carb} values were 0,26 mm/√days, 0,89 mm/√days and 1,74 mm/√days for ratio 0,4, 0,5 and 0,6 respectively.

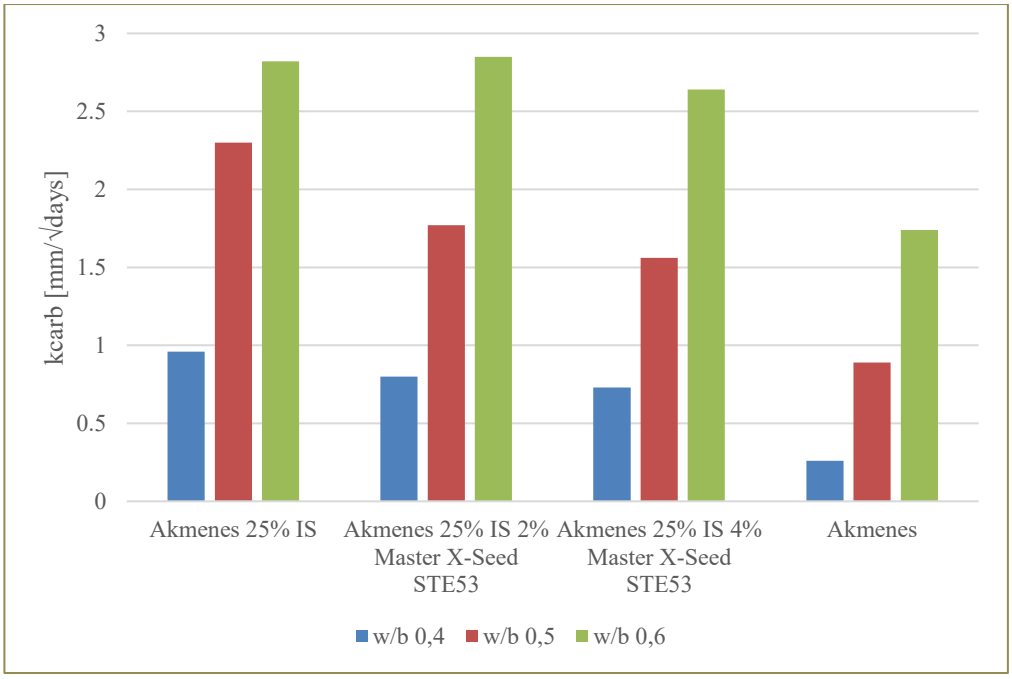

Figure 4-8 Carbonation coefficients k_{carb} for Akmenes mixes. All values for k_{carb} is shown in Appendix B1.

The results show that the inclusion of SEAs mostly have a positive impact when trying to reduce the carbonation coefficient in concrete with SCMs. A more pronounced effect could be seen for Akmenes mixes compared to the BAS VPI mixes when looking at w/b ratios 0,4 and 0,5. In the case of 2% Master X-Seed, Akmenes decrease 0,11 mm/√days more than BAS VPI for w/b ratio 0,4 and 0,46 mm/√days for w/b 0,5. In the case of 4% Master X-Seed STE53 k_{carb} decreases 0,12 mm/√days more for Akmenes than BAS VPI with a w/b ratio of 0,4 and 0,55 mm/√days more for w/b ratio 0,5. When looking at mixes with a w/b ratio of 0,6, Master X-Seed STE53 had a greater impact on BAS VPI as k_{carb} increased in Akmenes mixes with a 2% dosage, and for a 4% dosage k_{carb} decreased 0,21 mm/√days more for BAS VPI than Akmenes mixes.

4.3. Capillary Absorption

4.3.1. Capillary Absorption Coefficient k_{cap}

Using equation (3), the capillary absorption coefficient was calculated for all cementitious mixes.

The results for w/b ratio 0,4 for BAS VPI mixes shows several trends as well as irregularities regarding the influence of SEAs and SCMs on water absorption as seen in Figure 4-9. The reference mix without SEA (k_{cap} = 0,004930 kg/m^2√s) shows a comparatively moderate absorption rate. The adding of 2% Master X-Seed STE53 reduced the coefficient to 0,004195 kg/m^2√s, and further increasing the dosage to 4% resulted in an even lower value of 0,003618 kg/m^2√s, indicating improved resistance to capillary absorption with increasing SEA content. However, when 4% of Master X-Seed 100 was used instead, the coefficient slightly increased to 0,003967 kg/m^2√s, which is still better than the reference but not as effective as Master X-Seed STE53, suggesting a possible difference in performance between the two SEA types.

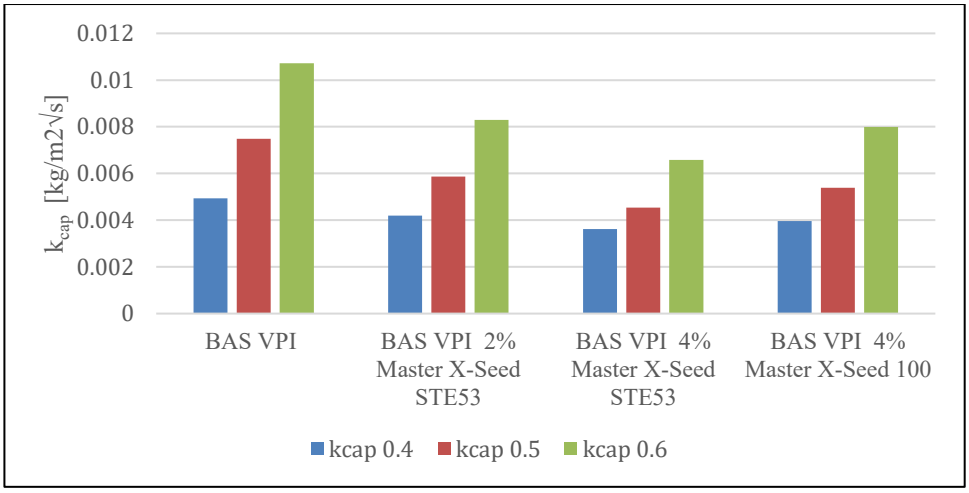

Figure 4-9 k_{cap} values for BAS VPI mixes. All values for k_{cap} is shown in Appendix C1 to C3.

The k_{cap} rates for w/b 0,5 have similar trends. However, they generally have shown higher absorption values. This is acceptable considering the higher water content in return increasing the porosity. The reference mix showed a k_{cap} value of 0,007483 kg/m^2√s which was significantly lowered with the addition of Master X-Seed STE53. A 2% dosage brought the value down to 0.005866 kg/m^2√s, and increasing the dosage to 4% further reduced it to 0,004541 kg/m^2√s, indicating that higher amounts of SEA continue to reduce the capillary absorption. However, replacing Master X-Seed STE53 with 4% X Seed 100 has increased k_{cap} of 0,005382 kg/m^2√s. This follows the earlier observation that Master X-Seed STE53 results in lower absorption compared to Master X-Seed 100.

The capillary absorption coefficients for the w/b 0,6 mixes indicated a clear increase in capillary activity compared to the 0,4 and 0,5 mixes, consistent with the expected trend of higher porosity at greater water content. The reference mix without any SEA showed a k_{cap} of 0,010716 kg/m^2√s. The introduction of 2% Master X-Seed STE53 reduced this to 0,008299 kg/m^2√s, and further increasing the SEA dosage to 4% brought it down significantly to 0,006577 kg/m^2√s, showing the beneficial effect of higher SEA content. However, the BAS VPI mix with 4% Master X-Seed 100 displayed a slightly higher coefficient of 0,007989 kg/m^2√s.

In the w/b ratio 0,4 Akmenes cement mixes with 25% IS as SCM, the reference mix showed the highest k_{cap} value of 0,007108 kg/m^2√s, see Figure 4-10. This value decreased with the inclusion of 2% and 4% Master X-Seed STE53 to 0,006244 kg/m^2√s and 0,005446 kg/m^2√s respectively, confirming the trend that higher SEA dosage improves capillary resistance even in SCM-rich mixes. Interestingly, the Akmenes mix without IS showed a high k_{cap} of 0,007226 kg/m^2√s, slightly higher than the IS mix.

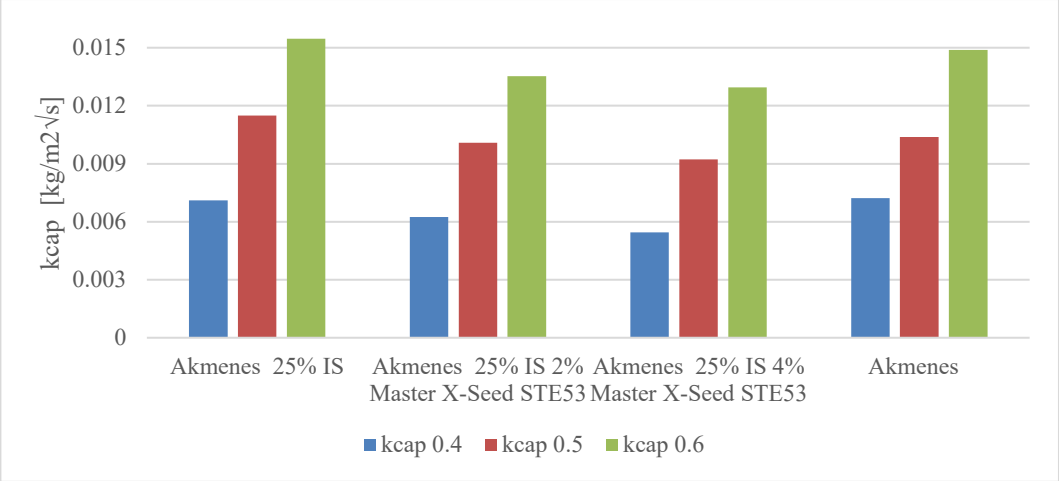

Figure 4-10 k_{cap} values for Akmenes mixes. All values for k_{cap} is shown in Appendix C1 to C3.

As for the w/b ratio 0,5 mixes, in the Akmenes cement mixes with 25% IS, the reference mix showed a very high k_{cap} value of 0,011485 kg/m^2√s, the highest among all mixes. The addition of Master X-Seed STE53 at 2% and 4% reduced this value to 0,010086 kg/m^2√s and 0,009219 kg/m^2√s, respectively, showing improvement. The Akmenes mix without IS also displayed a relatively high k_{cap} of 0,010384 kg/m^2√s, slightly lower than the IS-containing mix but still indicative of greater capillary activity.

Observing the w/b ratio 0,6 mixes, in Akmenes mixes with 25% IS, the reference mix showed a high k_{cap} of 0,015469 kg/m^2√s, which was partially mitigated by adding SEAs. A 2% Master X-Seed STE53 dosage brought the value to 0,013525 kg/m^2√s, while 4% reduced it further to 0,012943 kg/m^2√s. Although the trend of decreasing k_{cap} with increasing SEA dosage is consistent, the reduction is less pronounced compared to BAS VPI mixes. The Akmenes mix without IS is also showing a high k_{cap} of 0,014888 kg/m^2√s, slightly lower than the IS-containing reference, but still notably higher than the corresponding BAS VPI values.

4.3.2. Resistance Number m_{cap}

The resistance number m_{cap} for all cementitious mixes were calculated using equation (4).

Considering m_{cap} values of the w/b ratio 0,4 BAS VPI mixes, the following observation can be identified in Figure 4-11. The plain mix (no SEA) yielded a resistance number of $5{,}64\times10^7$ s/m², while adding 2% and 4% Master X-Seed STE53 slightly decreased the resistance to $5{,}23\times10^7$ and $5{,}25\times10^7$ s/m², respectively. Interestingly, the mix with 4% Master X-Seed 100 showed the lowest resistance of all at $5{,}10\times10^7$ s/m.

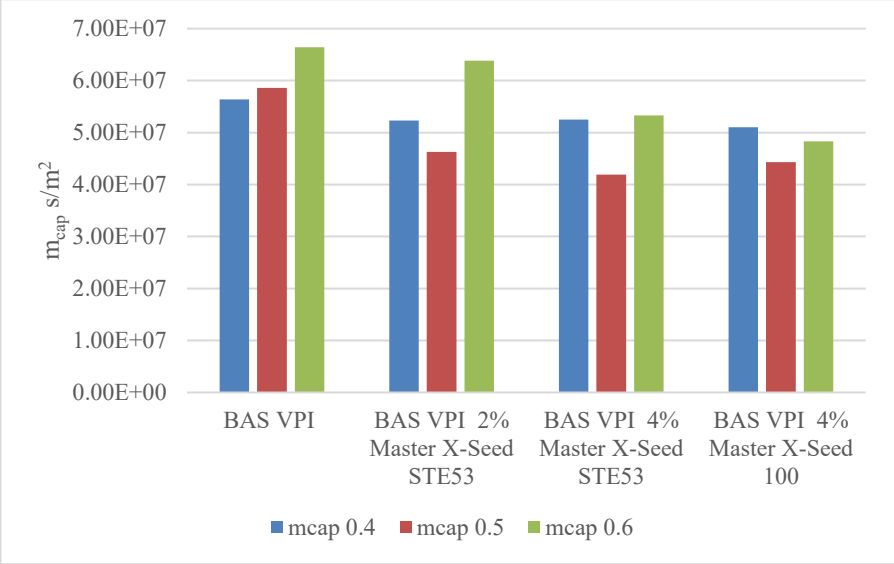

Figure 4-11 m_{cap} values for BAS VPI mixes. All values for m_{cap} is shown in Appendix C1 to C3.

The m_{cap} values of w/b ratio 0,5 mixes follow several of the w/b ratio 0,4 trends. The BAS VPI mix without SCMs or SEAs exhibited a resistance of $5{,}86\times10^7$ s/m², while the addition of 2% and 4% Master X-Seed STE53 reduced the m_{cap} values significantly to $4{,}63\times10^7$ and $4{,}19\times10^7$ s/m², respectively. But in contrast to w/b ratio 0,4 mixes, 4% Master X-Seed 100 showed a slightly higher m_{cap} of $4{,}43\times10^7$ s/m² compared to 4% Master X-Seed STE53.

In w/b ratio 0,6 mixes, the reference mix exhibited an m_{cap} of $6{,}64\times10^7$ s/m² in BAS VPI. The inclusion of 2% Master X-Seed STE53 led to a slight decrease to $6{,}38\times10^7$ s/m², while 4% Master X-Seed STE53 caused a more significant drop to $5{,}33\times10^7$ s/m². The mix with 4% Master X-Seed 100 further reduced the resistance to $4{,}83\times10^7$ s/m², showing irregularities with the earlier results.

In contrast to the w/b ratio 0,4 BAS VPI mixes, the Akmenes mixes with 25% IS content displayed significantly higher resistance numbers, see Figure 4-12, starting at 6,70×10⁷ s/m² for the reference mix without SEA. With the addition of 2% and 4% Master X-Seed STE53, the resistance increased further to 6,86×10⁷ and 6,23×10⁷ s/m², respectively. The Akmenes mix without IS maintained a high resistant value of 6,18×10⁷ s/m².

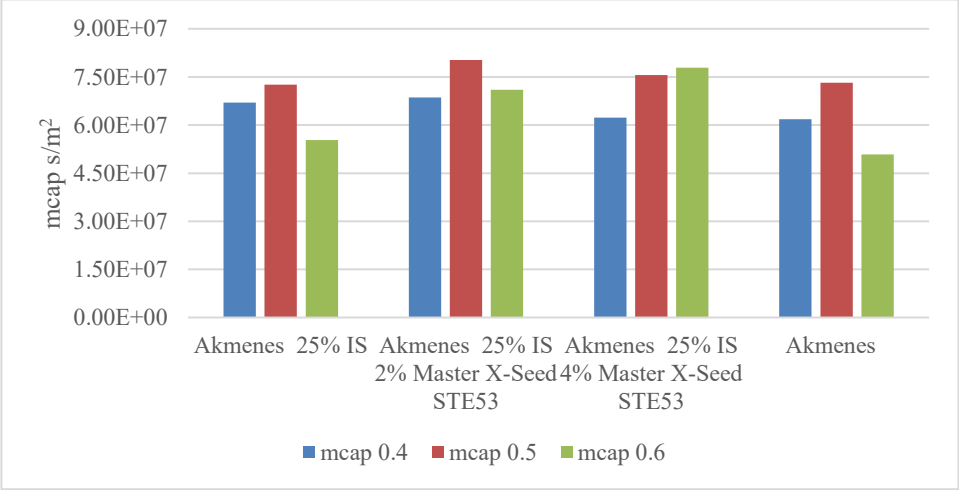

Figure 4-12 m_{cap} values for Akmenes mixes. All values for m_{cap} is shown in Appendix C1 to C3.

For w/b ratio 0,5, the Akmenes cement mixes showed consistently higher resistance numbers than BAS VPI. The reference mix with 25% IS showed 7,26×10⁷ s/m², and the inclusion of 2% and 4% Master X-Seed STE53 further increased the resistance to 8,03×10⁷ and 7,56×10⁷ s/m², respectively. The mix without IS still exhibited a relatively high m_{cap} of 7,32×10⁷ s/m².

In the case of Akmenes cement mixes of w/b ratio 0,6, results were more variable. The mix with 25% IS alone had an m_{cap} of 5,53×10⁷ s/m², but when 2% and 4% Master X-Seed STE53 were added, the resistance improved to 7,10×10⁷ and 7,79×10⁷ s/m², respectively. Interestingly, the Akmenes cement mix without IS displayed a lower m_{cap} of 5,08×10⁷ s/m².

4.3.3. Active Porosity

Using the water absorption measurements, the active and total porosity for all specimen were calculated. However, considering the scope and limitations of the study, Results for only Active Porosity was considered for analysis and comparisons. For comprehensive results of both active and total porosity, Appendixes C4, C5 and C6 can be referred to.

Active porosity represents the volume of capillary-accessible pores under normal submersion conditions and was calculated using the equation (8):

$$Active\ porosity = (V_{cap}) / V_{specimen} \times 100\% \qquad (8)$$

V_{cap} – Volume of water removed from capillary point to oven dry point
$V_{specimen}$ – Volume of Specimen

The porosity results for the mixes with a w/b ratio 0,4 are presented in Figure 4-13. The BAS VPI reference mix showed an active porosity of 10,71%. With the addition of 2% Master X-Seed STE53, active porosity slightly increased to 10,90%. However, at 4% Master X-Seed STE53 dosage, the value slightly decreased to 10,55%. A similar trend was observed with 4% Master X-Seed 100, which resulted in 10,85% active porosity, showing slightly lower total porosity compared to the 2% STE53 case, but marginally higher than the 4% STE53 mix.

For the w/b 0,5 mixes seen in Figure 4-13, the BAS VPI reference mix recorded an active porosity of 11,15%. When adding 2% Master X-Seed STE53, active porosity dropped to 10,06%, indicating pore refinement. At 4% Master X-Seed STE53, active porosity remained relatively low at 9,99%. The mix containing 4% Master X-Seed 100 showed higher porosity values than its STE counterpart, with active porosity at 10,78%.

For the w/b 0,6 series, porosity values increased overall due to higher water content as expected. The BAS VPI mix without SEA recorded an active porosity of 11,91%. The addition of 2% Master X-Seed STE53 decreased active porosity to 11,10%. A 4% SEA dosage further reduced active porosity to 10,13%. In the mix with 4% Master X-Seed 100, active porosity was 10,69%.

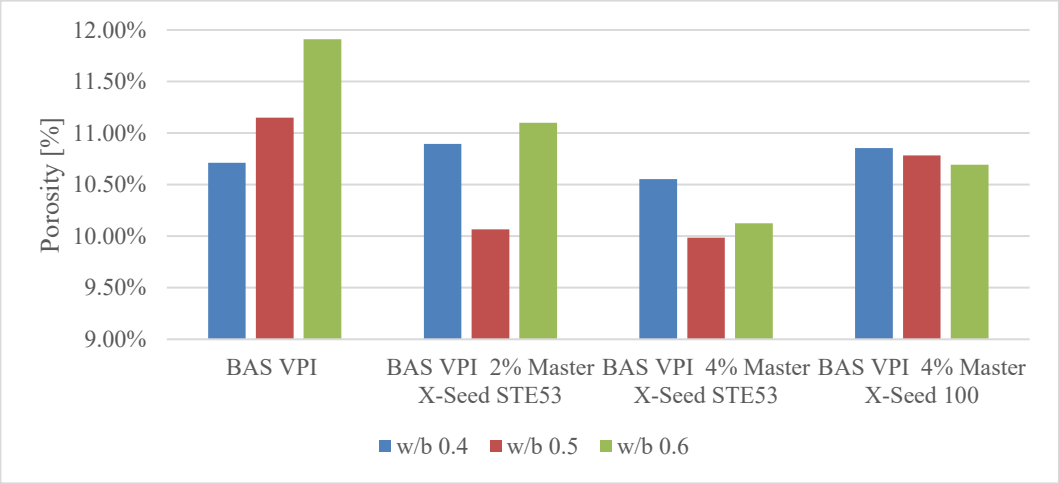

Figure 4-13 active porosity values for BAS VPI mixes. All values are shown in Appendix C4 to C6.

For the Akmenes cement-based mixes with 25% IS replacement and w/b ratio 0,4, the reference mix recorded an active porosity of 10,96%, as seen in Figure 4-14. When 2% Master X-Seed STE53 was added, active porosity decreased to 10,52%. A further increase to 4% SEA led to a more noticeable drop in active porosity to 9,78%. The Akmenes mix without IS had values of 10,60% active porosity.

In the w/b 0,5 series, the sample with 25% IS presented an active porosity of 12,35%. Adding 2% Master X-Seed STE53 led to a decrease the value, with active porosity at 11,51%. Increasing the dosage to 4% further reduced active porosity to 10,58%. The Akmenes mix without IS had an active porosity of 11,84%.

For the Akmenes cement mixes at w/b 0,6, the 25% IS mix exhibited an active porosity of 12,70%. With 2% Master X-Seed STE53, the values reduced slightly to 12,44%. At 4% Master X-Seed STE53, active porosity was nearly the same at 12,54%. The Akmenes mix without IS showed an active porosity of 12,43%.

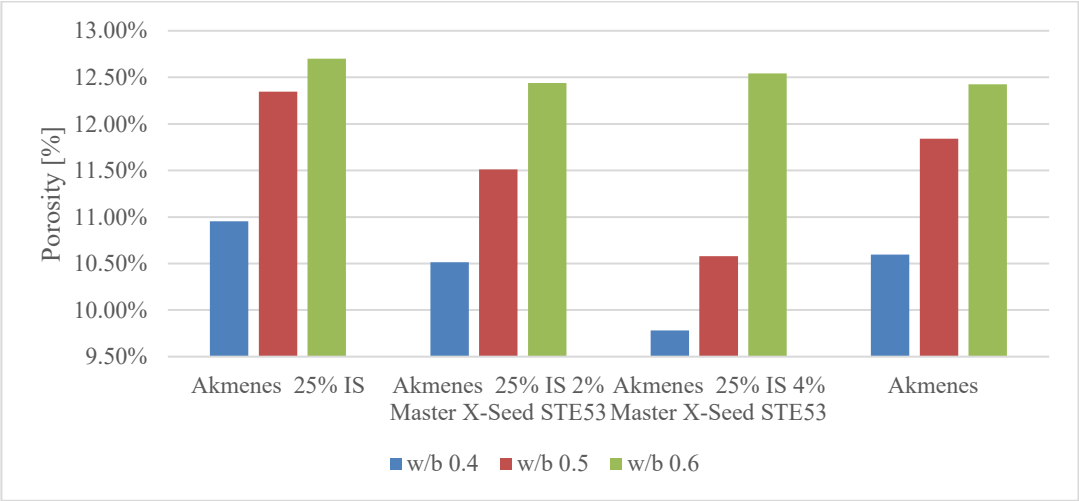

Figure 4-14 active porosity values for Akmenes mixes. All values are shown in Appendix C4 to C6.

5. Result Analysis and Discussion

The first aim of this study was to evaluate whether there is a relationship between carbonation behavior and other key parameters, specifically compressive strength and capillary absorption characteristics. Accordingly, a correlation analysis was first performed between carbonation coefficient and compressive strength (see Section 5.1), followed by an analysis of the correlation between carbonation coefficient and various capillary absorption indicators, namely, capillary absorption coefficient, resistance number, active porosity, and total porosity (see Section 5.2).

To determine whether these relationships are statistically significant, the coefficient of determination (R^2) were used. The R^2 value quantifies the proportion of variance in the dependent variable that is explained by the independent variable(s) in a regression model. An R^2 value closer to 1 indicates a strong linear correlation, while values below 0.3 suggest a negligible relationship [37].

Following the correlation analysis, the effect of incorporating SCMs on carbonation resistance was evaluated by comparing mixes with and without SCMs across different w/b ratios (see Section 5.3). Next, the influence of SEAs on carbonation resistance, later age compressive strength and capillary absorption was investigated (see Section 5.4). Even though an analysis of variance (ANOVA) is recommended for this, we had to use a regression analysis instead due to the availability of only single average values for k_{carb}, compressive strength and capillary absorption parameters.

Finally, a comparative evaluation was conducted between two types of strength enhancers, Master X-Seed 100 and Master X-Seed STE53, to better understand their relative impact on carbonation performance (see Section 5.5).

5.1. Correlation between Compressive Strength and Carbonation

The correlation analysis between compressive strength and carbonation was carried out separately for the BAS VPI and Akmenes mixes. This was to get a more accurate correlation, as the different SCMs have different replacement percentages and chemical compositions, and the BAS VPI and Akmenes mixes will therefore have a different correlation between compressive strength and carbonation rate. 4 scatterplots were made containing all mixes of each cement (except for Akmenes with no SCM), one for 28 days testing and one for 56 days testing for each cement.

Figure 5-1 shows that the correlation between k_{carb} and compressive strength at 28 days for BAS VPI mixes was very high, with a R^2 value of 0,97. The graph shows that compressive strength decreases with an increased k_{carb}, with the highest compressive strength being 76,4 MPa for the mix with w/b ratio 0,4 and 2% Master X-Seed STE53, which simultaneously had the second lowest k_{carb} of 0,63 mm/$\sqrt{}$ days. The lowest compressive strength at 37,9 MPa was measured for the mix with a w/b ratio 0,6 and no SEA, which also had the highest carbonation rate at 2,25 mm/$\sqrt{}$ days. The results of the other mixes generally follow the same pattern with slight deviations from the regression line.

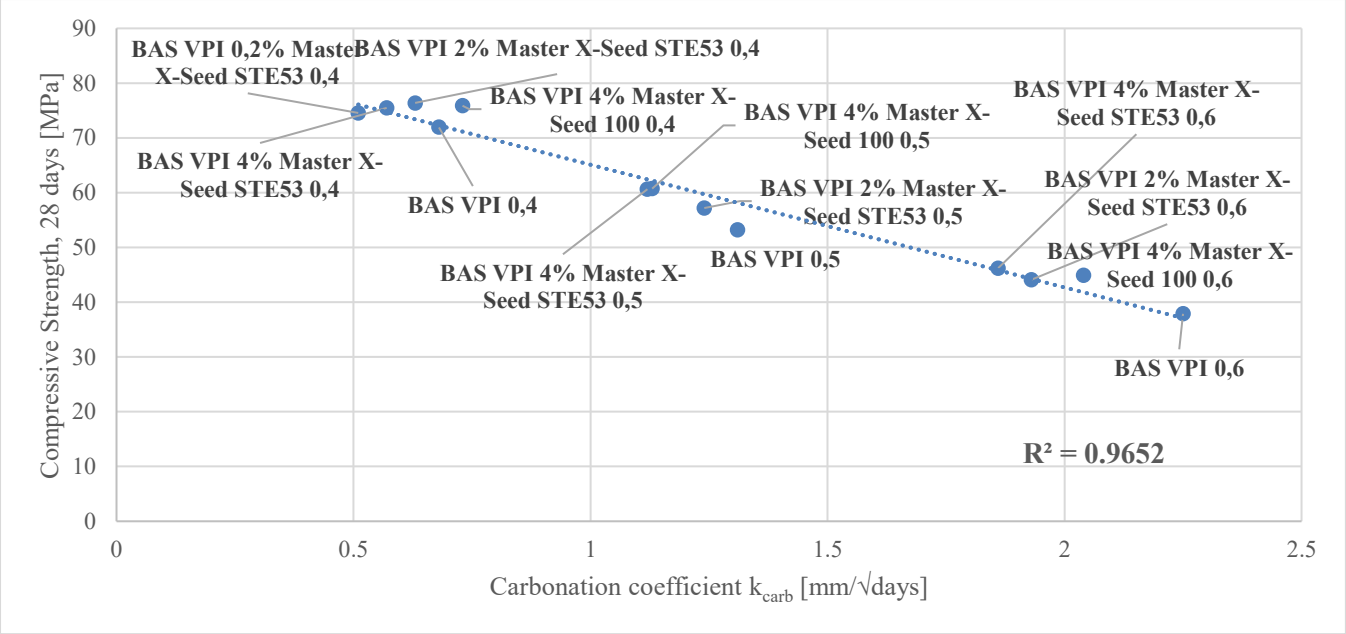

Figure 5-1 Correlation between carbonation coefficient and compressive strength after 28 days for BAS VPI. The values for BAS VPI compressive strength and k_{carb} are found in Appendix A1 and B1, respectively.

When comparing k_{carb} to compressive strength after 56 days of curing, the correlation was weaker with a R^2 value of 0,86. This is likely due to the inconsistent results where the compressive strength decreased for the mixes with no SEA and 2% Master X-Seed STE53, w/b ratio 0,4. As can be seen in Figure 5-2, the mix with w/b 0,4 and no SEA is deviating significantly from the regression line, causing the lower R^2 value.

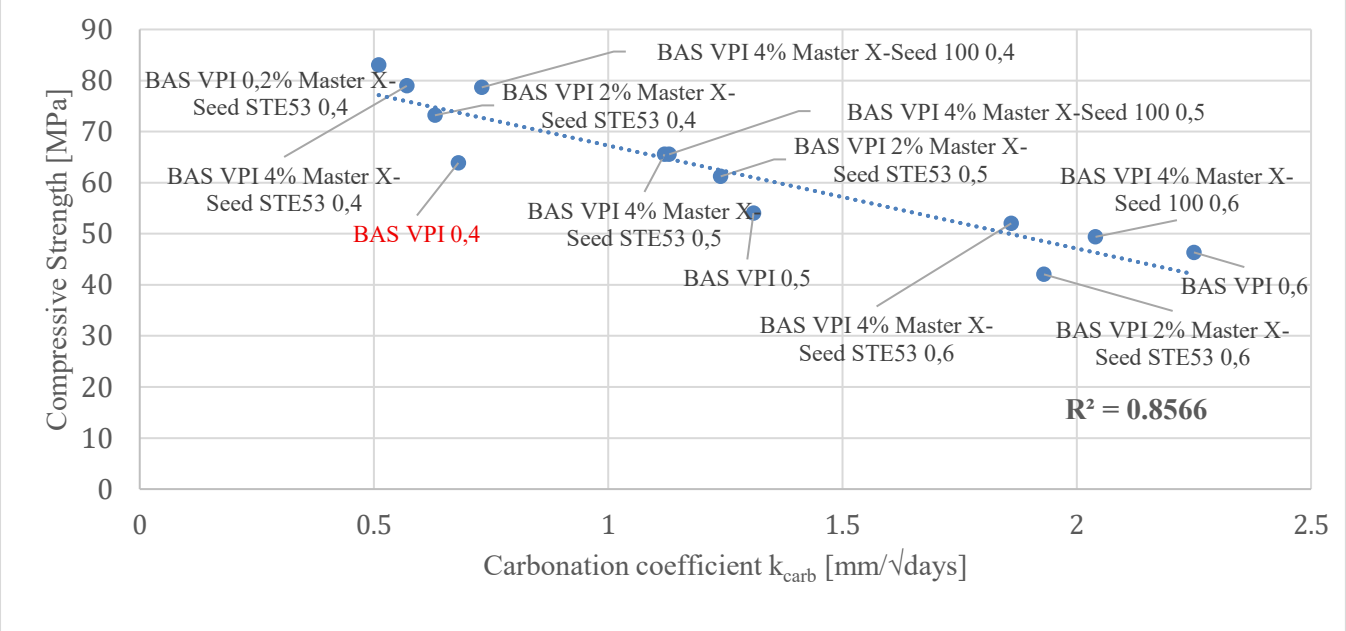

Figure 5-2 Correlation between carbonation coefficient and compressive strength after 56 days for BAS VPI. The values for BAS VPI compressive strength and k_{carb} are found in Appendix A1 and B1, respectively.

The correlation between carbonation rates and compressive strength were also almost linear for the Akmenes mixes. For the 28 days compressive tests, the R^2 value was 0,96, and the same pattern that was seen for BAS VPI mixes is seen for these mixes. Figure 5-3 shows that increased carbonation rates lead to decreased compressive strength, but the carbonation rates are higher (between 0,73 mm/√days and 2,85 mm/√days) and the strengths lower (between 28,1 MPa and 64,3 MPa) than for the BAS VPI mixes.

The mixes with no IS or SEA have been filtered out as they will deviate substantially from the regression line and doesn't show the effect of the SEA or IS.

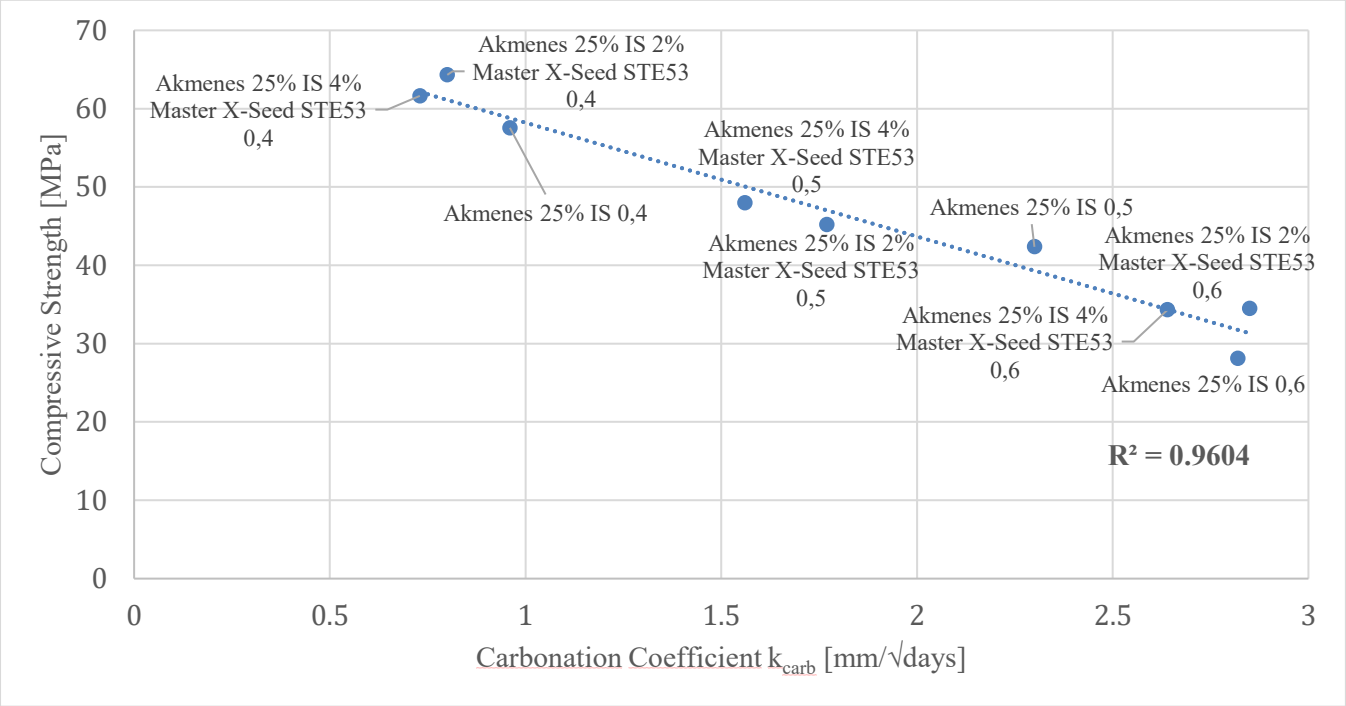

Figure 5-3 Correlation between carbonation coefficient and compressive strength after 28 days for Akmenes. The values for Akmenes compressive strength and k_{carb} are found in Appendix A2 and B1 respectively.

The correlation for 56 days compressive strength results was almost as high, with a R^2 value of 0,95. The only difference from the 28 days test is that the mix with 25% IS and no SEA and a w/b ratio of 0,4 deviated slightly more from the regression line as seen in Figure 5-4.

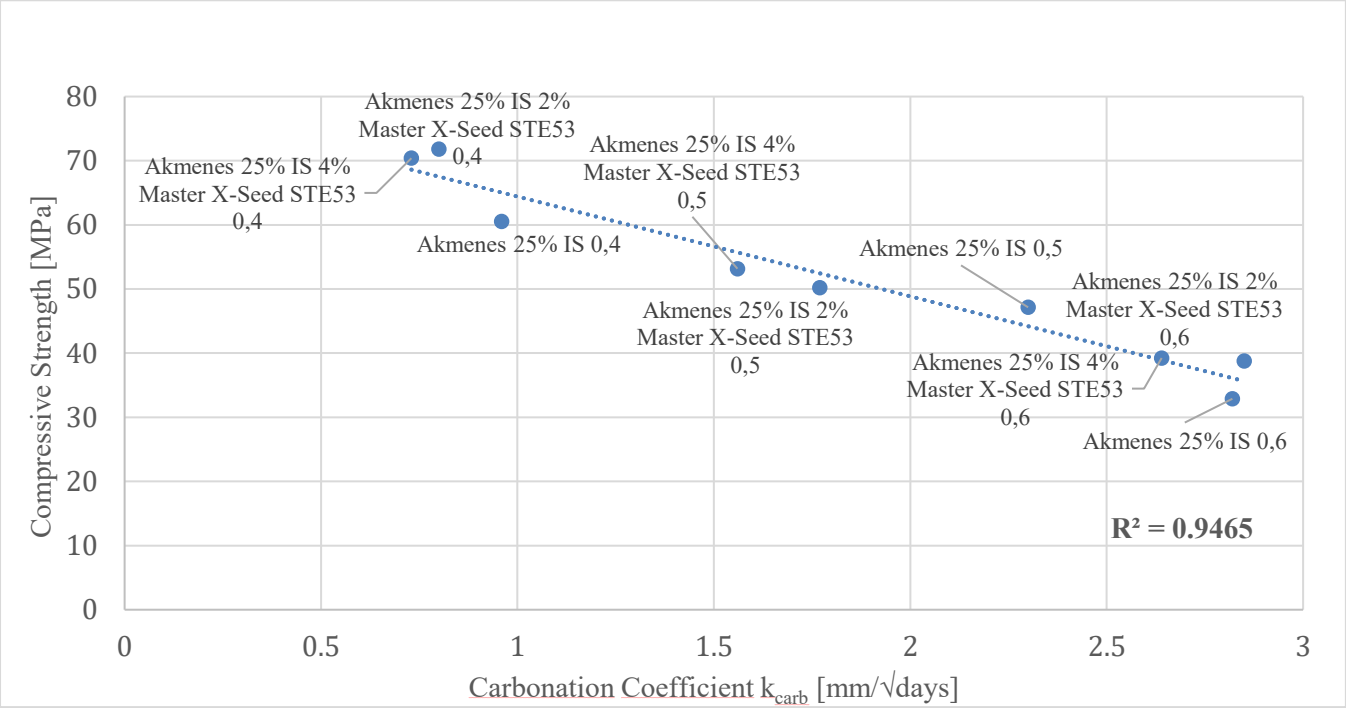

Figure 5-4 Correlation between carbonation coefficient and compressive strength after 56 days for Akmenes. The values for Akmenes compressive strength and k_{carb} are found in Appendix A2 and B1 respectively.

The high R^2-values for the comparison between compressive strength and carbonation rates supports the idea that the relationship between compressive strength and carbonation is approximately linear, as mentioned in section 1.1.3. The main reason for this is likely the porosity of the concrete, as it can be seen in the graphs that carbonation rates are increased and compressive strength decreased with an increased w/b ratio. This is due to a less dense microstructure leading to both an increased permeability of CO_2 and a less compact concrete mix.

As stated before, the pure Akmenes cement mixes were removed from the correlation analysis as they deviated significantly from the regression line. A reason for this may be that as the concrete mixes do not contain any SCMs therefore contain more Portland cement and subsequently more $Ca(OH)_2$ which leads to a smaller reduction in pH value, lower carbonation rates and higher compressive strengths. The improvement in compressive strength was however low compared to the decrease of carbonation rates, as can be seen in sections 4.1 and 4.2. This leads to the mixes deviating significantly from the regression line.

The reason for the lower R^2 value for BAS VPI mixes and 56 days compressive strength testing is likely poor compaction of the mixes with no SEA and with 2% Master X-Seed STE53 and w/b ratio 0,4. This leads to a less favorable microstructure of the concrete with risk for entrapped air and increased porosity and therefore reduced compressive strength.

5.2. Correlation between Capillary Absorption and Carbonation

To investigate the relationship between capillary absorption and carbonation, scatter plots were drawn by having k_{carb} in the x axis while plotting the capillary absorption coefficients (k_{cap} and m_{cap}) in the y axis. A scatter plot for each w/b ratio was created, which enabled visual representation and helped in identifying correlations. Then the R^2 value was calculated to understand the correlation between the coefficients.

5.2.1. Capillary Coefficient vs Carbonation

When all eight data points (the 8 mixes of 0,4 w/b ratio) were included in the analysis, the calculated R^2 value was extremely low at 6×10^{-6}, indicating virtually no linear correlation between k_{cap} and k_{carb}. This poor correlation was primarily influenced by the presence of an outlier—the Akmenes mix without IS. This mix exhibited the highest capillary coefficient (0,0072 kg/m$^2\sqrt{s}$) but an unexpectedly low k_{carb} of 0,26 mm/$\sqrt{}$days, which significantly deviated from the general trend observed in the other mixes. Therefore, this mix was removed as it misrepresents the correlation. After removing this outlier, the R^2 value improved substantially to 0,82 as seen in Figure 5-9, suggesting a strong positive correlation between capillary absorption and carbonation behavior across the remaining data. This trend helps to build the relationship where increased capillary porosity improves CO_2 ingress, thereby enhancing carbonation rates. For example, mixes with higher k_{cap} demonstrates higher k_{carb} values. Whereas mixes with lower k_{cap} such as BAS VPI 4% Master X-Seed STE53 show lower k_{carb} values.

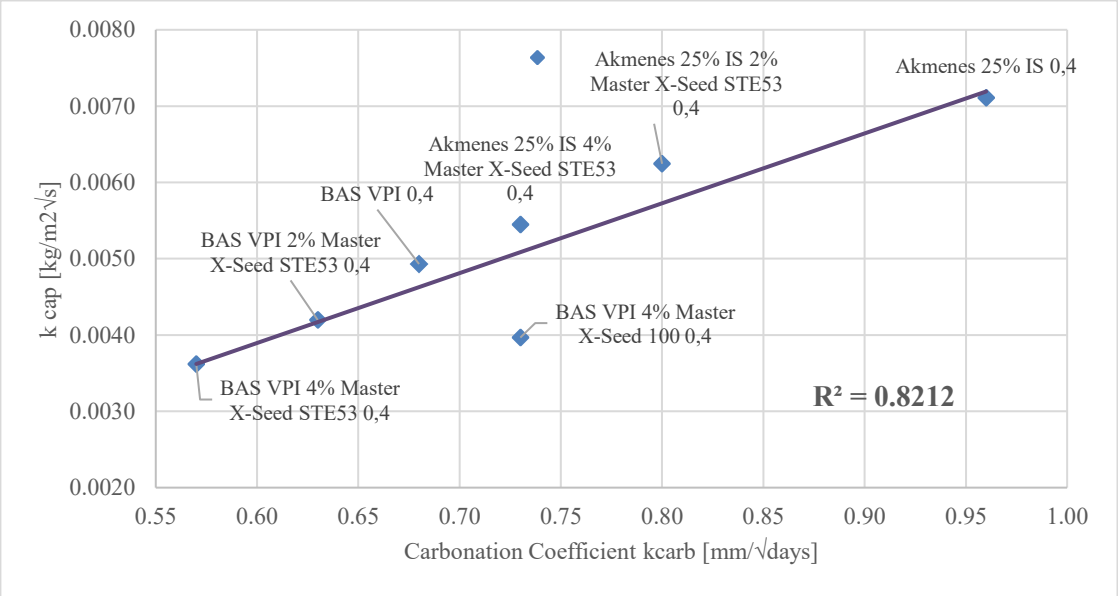

Figure 5-5 Correlation between k_{carb} and k_{cap} for w/b 0,4. Values for k_{carb} and k_{cap} are found in Appendix B1 and C1, respectively.

The linear relationship between k_{cap} and k_{carb} was evaluated for the w/b ratio 0,5 mixes. The R^2 value was 0,89 as seen in Figure 5-6, revealing a strong positive correlation between k_{cap} and k_{carb} for the remaining mixes. This indicates that higher capillary absorption is generally associated with higher carbonation depth development, aligning with theoretical expectations.

Within the BAS VPI series, the trend was consistent: increasing the dosage of Master X-Seed STE53 reduced both k_{cap} (from 0,0075 kg/m^2√s to 0,0045 kg/m^2√s) and k_{carb} (from 1,31 mm/√days to 1,12 mm/√days). The BAS VPI mix with 4% Master X-Seed 100 followed a similar pattern with a k_{cap} of 0,0054 kg/m^2√s and k_{carb} of 1,13 mm/√days. For the Akmenes cement mixes containing 25% IS, a clear reduction in both k_{cap} and k_{carb} was also observed as the SEA dosage increased—from k_{cap} 0,0115 kg/m^2√s to 0,0092 kg/m^2√s and k_{carb} from 2,30 mm/√days to 1,56 mm/√days.

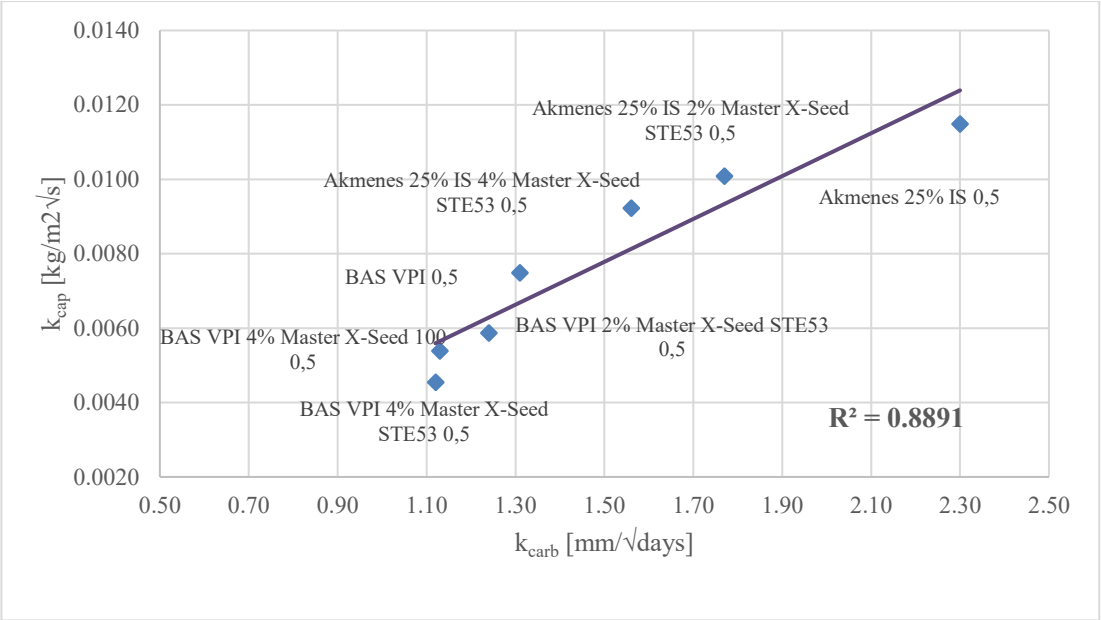

Figure 5-6 Correlation between k_{carb} and k_{cap} for w/b 0,5. Values for k_{carb} and k_{cap} are found in Appendix B1 and C2, respectively.

In the w/b 0,6 scatter plot, the R^2 exhibited a value of 0,94 as seen in Figure 5-7, indicating a very strong linear relationship between k_{cap} and k_{carb} for the remaining mixes. This result clearly supports the idea that increased k_{cap} is closely linked to higher carbonation depth, likely due to the more open and accessible pore structure that facilitates CO_2 ingress.

In the BAS VPI group, the trend was clear—k_{cap} decreased from 0,0107 to 0,0066 kg/m^2√s as the dosage of Master X-Seed STE53 increased, and k_{carb} reduced as well from 2,25 to 1,86 mm/√days. The mix with 4% Master X-Seed 100 showed slightly higher values (k_{cap} = 0,0080 kg/m^2√s and k_{carb} = 2,04 mm/√days) compared to its STE53 counterpart. For the Akmenes cement mixes with 25% IS, the correlation was also strong: mixes with higher k_{cap} values (like 0,0155 kg/m^2√s) corresponded with higher k_{carb} values (2,82 mm/√days), and those with reduced k_{cap} had lower carbonation depths.

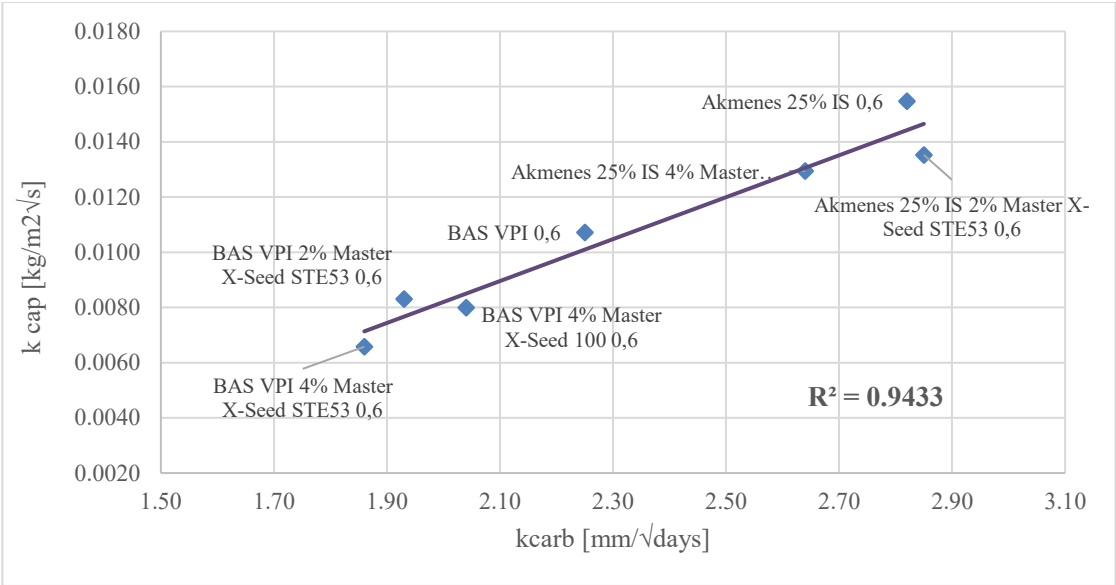

Figure 5-7 Correlation between k_{carb} and k_{cap} for w/b 0,6. Values for k_{carb} and k_{cap} are found in Appendix B1 and C3, respectively.

5.2.2. Resistance Number vs Carbonation

For the w/b 0,4 mixes, the initial correlation between k_{carb} and m_{cap} was very weak, with an R^2 value of 0,0967. However, as evident in the results from k_{cap} The Akmenes 0,4 mix without SCM was influencing heavily towards making the correlation weak, showing a low k_{carb} (0,26 mm/√days) despite a high m_{cap} value ($6{,}2\times10^7$ s/m²).

Upon removing this outlier, the R^2 value increased to 0.61 as seen in Figure 5-8, indicating a moderate correlation. However, due to the small sample size and variability in binder systems, this trend alone is insufficient to draw a reliable relationship between k_{carb} and m_{cap}.

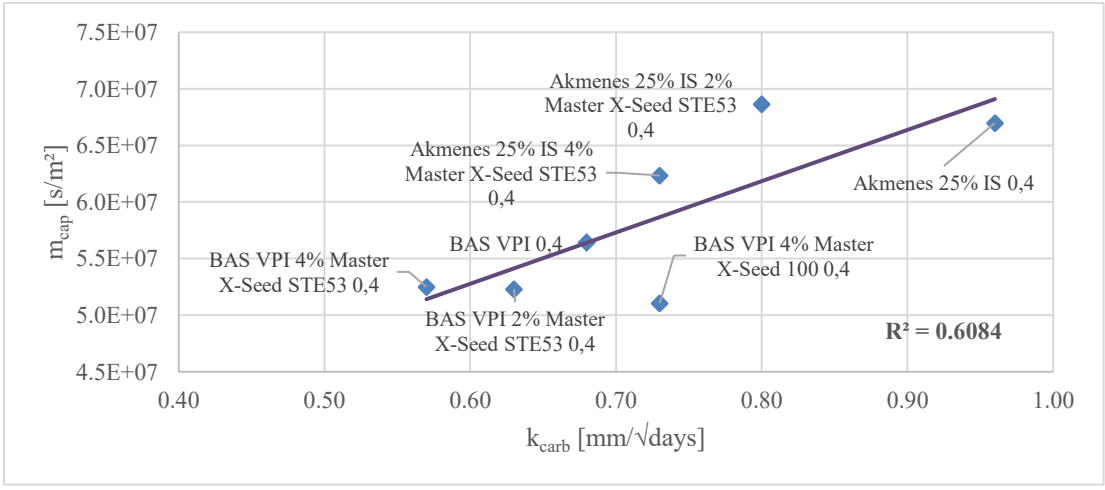

Figure 5-8 Correlation between k_{carb} and m_{cap} for w/b 0,4. Values for k_{carb} and m_{cap} are found in Appendix B1 and C1, respectively.

In the w/b 0,5 group, the R^2 value was 0,63 as seen in Figure 5-9. There is no strong or consistent linear relationship between k_{carb} and m_{cap} for these mixes.

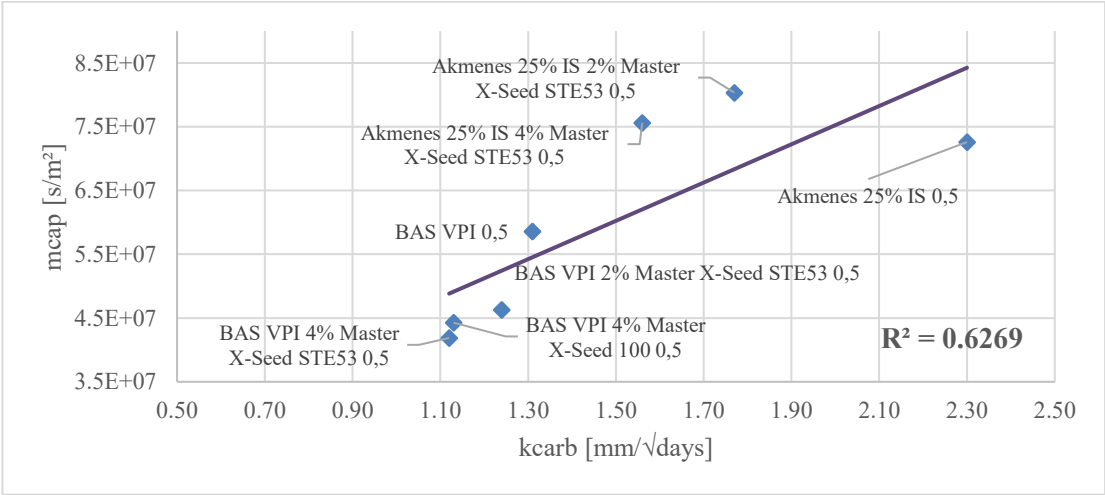

Figure 5-9 Correlation between k_{carb} and m_{cap} for w/b 0,5. Values for k_{carb} and m_{cap} are found in Appendix B1 and C2, respectively.

For mixes with w/b 0,6, the R^2 value was 0,25 as seen in Figure 5-10, suggesting a weak connection between the two parameters. Overall, the relationship remains inconsistent across the dataset.

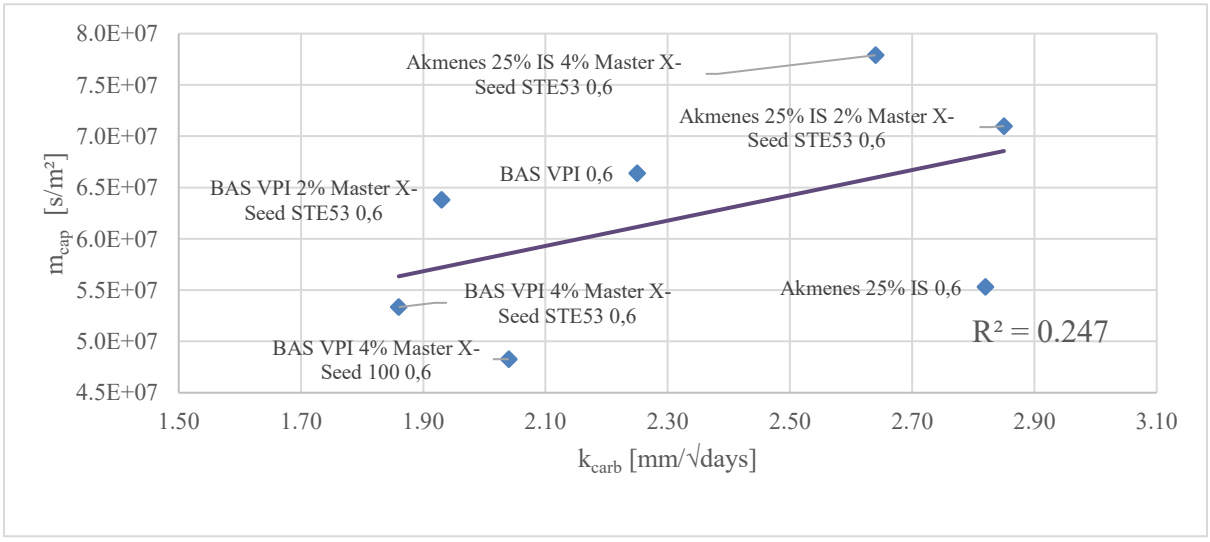

Figure 5-10 Correlation between k_{carb} and m_{cap} for w/b 0,6. Values for k_{carb} and m_{cap} are found in Appendix B1 and C3, respectively.

These results show that while some moderate trends exist between carbonation coefficient and m_{cap} in subsets of the data, no strong or consistent correlation could be established across all mixes. This suggests that m_{cap} alone is not a reliable predictor of carbonation resistance,

especially given the varying effects of SCM types, binder composition, and admixture interactions.

Moreover, outliers such as mixes without SCMs particularly those with higher $Ca(OH)_2$ content appear to behave differently in terms of carbonation, despite having similar m_{cap} values.

5.2.3. Active Porosity vs Carbonation

The relationship between k_{carb} and active porosity was examined across mixes with w/b ratios 0,4, 0,5 and 0,6 to assess whether the volume of capillary-accessible pores correlates with carbonation resistance. For all plots, the Akmenes mix without SCM was excluded.

For the w/b ratio 0,4, the results revealed virtually no linear correlation with a R^2 value of 0,025 as seen in Figure 5-11, suggesting that active porosity does not significantly influence carbonation in this case.

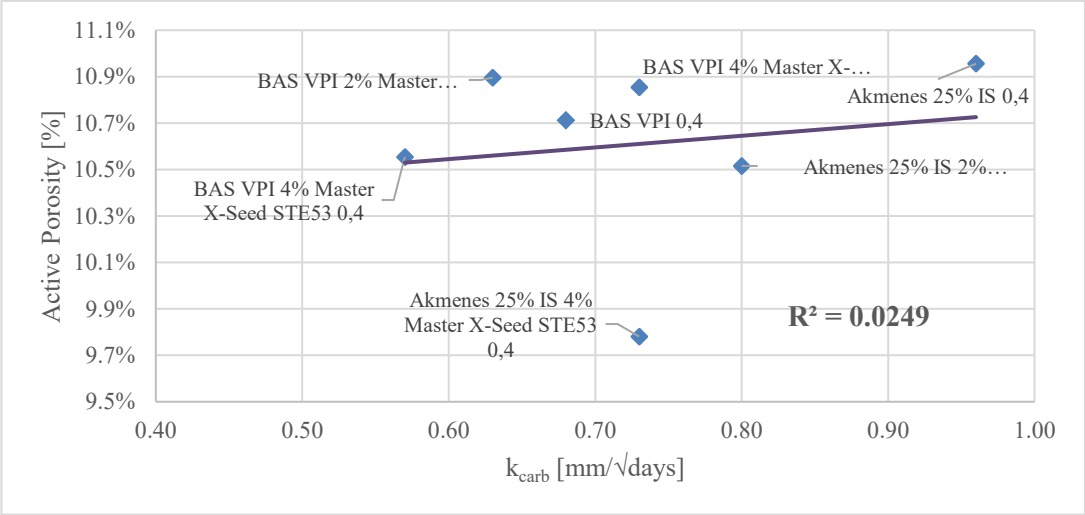

Figure 5-11 Correlation between k_{carb} and active porosity for w/b 0,4. Values for k_{carb} and active porosity are found in Appendix B1 and C4, respectively.

In contrast, the mixes with w/b 0,5 showed an improved correlation. The R^2 exhibited a value of 0,76 as seen in Figure 5-12. This indicates a comparatively stronger linear relationship between active porosity and carbonation rate, suggesting that as active porosity decreases, carbonation resistance improves especially when the w/b ratio is comparatively higher.

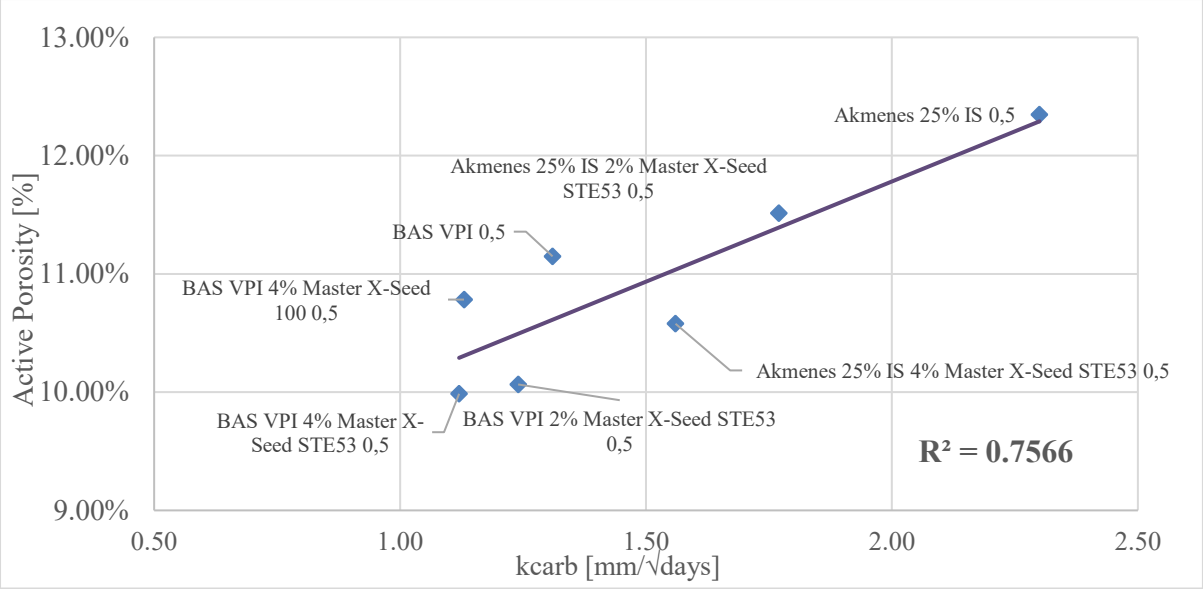

Figure 5-12 Correlation between k_{carb} and active porosity for w/b 0,5. Values for k_{carb} and active porosity are found in Appendix B1 and C5, respectively.

When the w/b 0,6 ratio results were plotted the R^2 value showed 0,87 as seen in Figure 5-13. This again points to a clearer correlation between increased active porosity and higher carbonation coefficients when the dataset is consistent and the w/b ratio is increased.

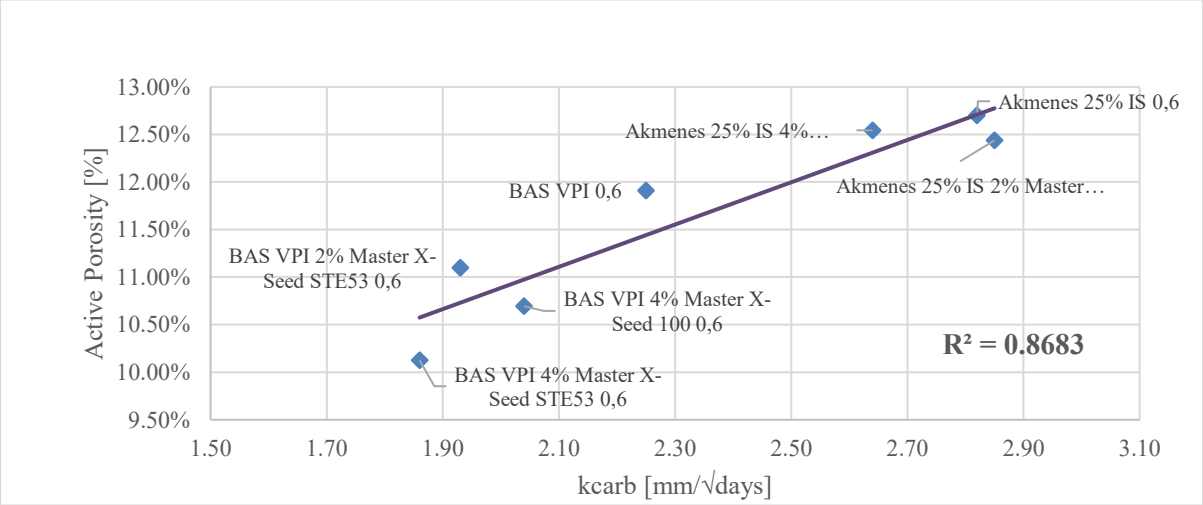

Figure 5-13 Correlation between k_{carb} and active porosity for w/b 0,6. Values for k_{carb} and active porosity are found in Appendix B1 and C6, respectively.

These findings highlight that while active porosity alone is not always a strong predictor of carbonation rate, especially at lower w/b ratios, it becomes more relevant at higher water contents—provided that mixes without SCMs and SEAs are filtered out. Outliers like the Akmenes mixes may behave differently due to factors such as high $Ca(OH)_2$ content or specific pore structures that slow carbonation despite higher water absorption. This emphasizes the need to consider both quantitative porosity factors and microstructural characteristics when trying to build a full picture with carbonation.

Across the three capillary-transport descriptors tested, k_{cap} emerged as the most consistent proxy for k_{carb} when the dataset is coherent. After removing the Akmenes outlier with no SCM,

the k_{cap}–k_{carb} relationship was strong at every w/b: $R^2 \approx 0,82$ (0,4), 0,89 (0,5) and 0.94 (0,6). Within both cementitious systems, raising SEA dosage lowered k_{cap} and was accompanied by a reduction in k_{carb}. This co-variation supports the overall expectation: mixes that absorb water faster through capillaries also tend to admit CO_2 more readily.

By contrast, m_{cap} showed inconsistent correlation with carbonation. Even after excluding the outlier, correlations were only moderate at w/b 0,4–0,5 ($R^2 \approx 0,61$–$0,63$) and negligible at w/b 0,6 ($R^2 \approx 0,25$). Practically, m_{cap} depends on identifying t_{cap} , the transition from capillary to diffusion, whose placement is method-sensitive and influenced by factors not directly governing gaseous CO_2 ingress. In practice we referred to ASTM C1585, which treats the initial capillary absorption window as up to 6 h. However, a fixed 6 h is not universally valid: the true capillary period varies by mix, w/b ratio, curing, and the presence of SCMs/SEAs—all of which shift the change of slope. This explains the non-consistent correlations we observed versus carbonation. This makes m_{cap} a less reliable predictor of k_{carb} than k_{cap}.

The active porosity and k_{carb} relation depended on w/b. At w/b 0,4, the correlation was negligible ($R^2 \approx 0,025$), but it strengthened markedly at higher w/b: 0,76 (0,5) and 0,87 (0,6). At elevated water contents, variability in the fraction of capillary-accessible voids appears to dominate ingress, so active porosity tracks carbonation better. At lower w/b, other influences (binder chemistry, degree of hydration, curing) obstruct a simple porosity–carbonation correlation.

The recurring outlier Akmenes without SCM/SEA—had high absorption yet low k_{carb}. This is plausibly explained by its higher portlandite availability (no SCM consumption of $Ca(OH)_2$), which buffers pH and slows carbonation progression [38], despite relatively rapid water uptake. Once such mixes were excluded, the dataset behaved generally consistently as expected.

5.3. Carbonation of Cementitious Systems with SCMs

The influence of SCMs on carbonation behavior was investigated by comparing mixes with and without SCMs across different w/b ratios. Due to limitations in the mix design matrix, and the fact that one of the two main cements used (BAS VPI) already contains a blended SCM, the comparison was narrowed to only two cementitious systems:

Akmenes cement without SCMs (0,4, 0,5, 0,6)
Akmenes cement with 25% IS as SCM (0,4, 0,5, 0,6)

The carbonation coefficients k_{carb} for these six mixes were plotted on the same graph to directly compare the effect of SCM inclusion at three w/b ratios (0,4, 0,5, and 0,6) ,see Figure 5-14. The results reveal a clear and consistent trend across all w/b levels.

For the non-SCM Akmenes mixes, the carbonation coefficients increased with higher water content, ranging from 0,26 mm/√days at w/b 0,4 to 1,74 mm/√days at w/b 0,6. This trend aligns with expectations, as higher w/b ratios generally lead to increased porosity and faster carbonation due to greater CO_2 diffusivity.

However, for the SCM-included mixes (with 25% IS), carbonation rates were significantly higher at every w/b ratio: At w/b 0,4 carbonation increased significantly from 0,26 to 0,96 mm/√days, at w/b 0,5 from 0,89 to 2,30 mm/√days, and at w/b 0,6 from 1,74 to 2,82 mm/√days

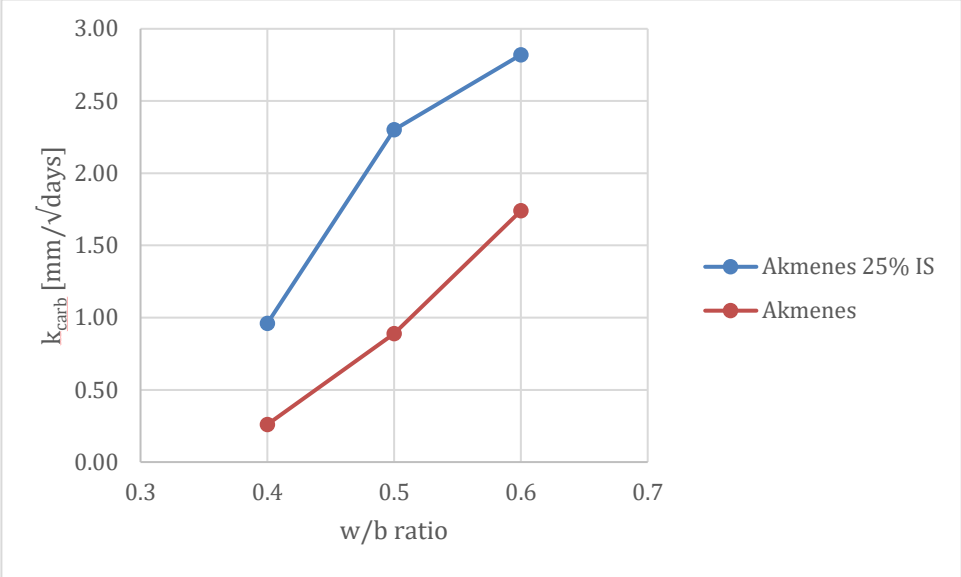

Figure 5-14 Akmenes vs Akmenes 25% IS Carbonation. k_{carb} values can be found in Appendix B1.

These results clearly indicate that the inclusion of 25% IS as an SCM increases the carbonation rate. A reason for this effect can be the reduction in $Ca(OH)_2$ in the mix when SCMs are used. IS, like many SCMs, consumes $Ca(OH)_2$ through pozzolanic reactions. As a result, CO_2 is able to reduce the pH of the pore solution more quickly, allowing carbonation to proceed more rapidly, even if the permeability is not significantly higher.

The result contradicts the previous study by Shi et.al. (2008) that reported that the usage of copper slag (iron silicates) had a positive effect on the carbonation of concrete and slowing down the carbonation rate. However, it should be noted that in Shi et.al. (2008), copper slag was used as a fine aggregate replacement. Also, the copper slag used in that study might not have had the same material chemistry as the Iron Silicate used in this study. Furthermore, since carbonation is calculated using the depth which depends on the personal and instrumental accuracy, there could have been differences in results.

5.4. Addition of SEAs to BAS VPI Cementitious systems

In addition to SCMs, SEAs were incorporated into selected cementitious systems to evaluate their effect on carbonation resistance, capillary absorption and compressive strength. As only three mixes used Master X-Seed 100 (BAS VPI, 4%), this analysis focuses solely on the influence of Master X-Seed STE53, tested at two dosage levels: 2% and 4%. (with the reference mix being used as 0%)

The comparison was carried out separately for the BAS VPI system, which already contains SCMs in the binder, and the Akmenes cement system with 25% IS. In both cases, mixes with 0%, 2%, and 4% Master X-Seed STE53 were analyzed across three w/b ratios (0,4, 0,5, and 0,6).

5.4.1. SEA effect on carbonation

In the BAS VPI system, the addition of Master X-Seed STE53 resulted in a consistent reduction in k_{carb} at all w/b ratios as seen in Figure 5-15. From the reference mixes with no SEA to those with 4% SEA, a steady decline in k_{carb} was observed. This indicates that Master X-Seed STE53 contributes positively to carbonation resistance, likely due to accelerated hydration and pore refinement, which together densifies the matrix and hinders CO_2 penetration. The reduction in carbonation was most notable at lower w/b ratios, where the effect of admixtures is more effectively understood due to less capillary porosity.

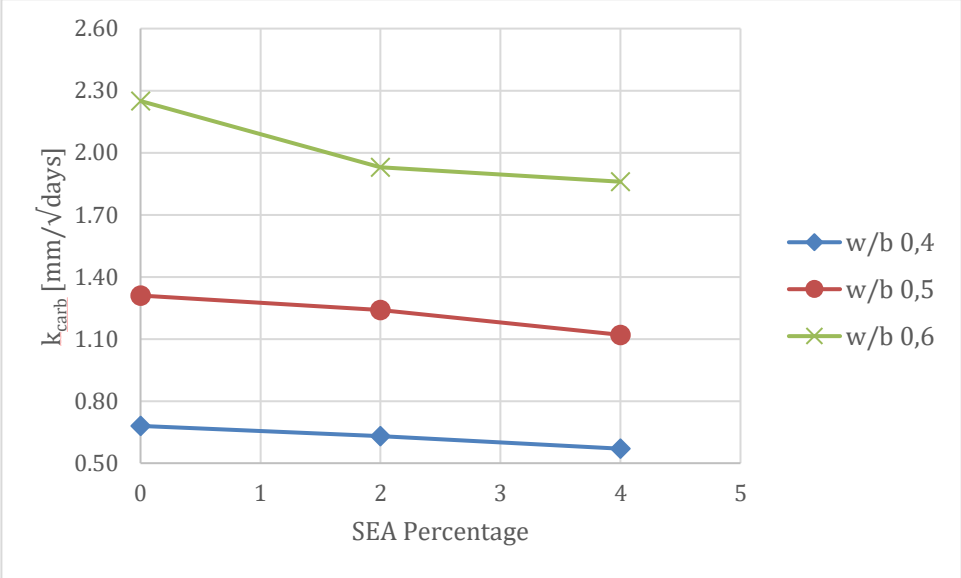

Figure 5-15 BAS VPI Carbonation with increasing SEA percentage. k_{carb} values can be found in Appendix B1.

For the Akmenes cement mixes with 25% IS, a similar trend was observed, see Figure 5-16. Increasing the SEA dosage from 0% to 4% generally led to lower k_{carb}, particularly at w/b ratios of 0,4 and 0,5. However, at w/b 0,6, the k_{carb} slightly increased with 2% SEA before decreasing again at 4%. This irregularity could be a result from the higher inherent porosity at w/b 0,6, where the effect of SEA may be less dominant or factored less by the more porous structure. Nonetheless, the overall performance with 4% SEA was better than the reference value, reinforcing the durability benefit at higher admixture levels.

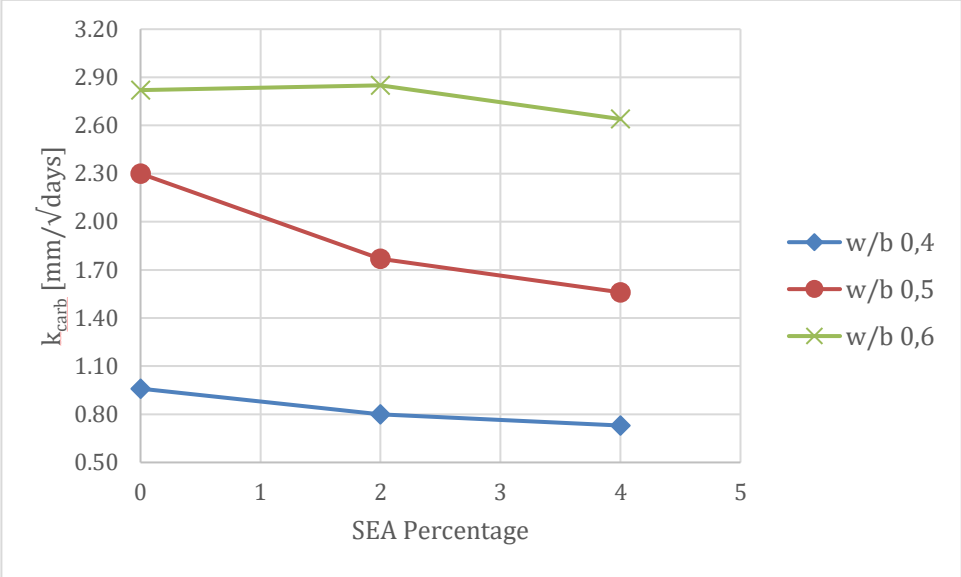

Figure 5-16 Akmenes 25% IS with increasing SEA percentage. k_{carb} values can be found in Appendix B1.

These findings demonstrate that Master X-Seed STE53 can enhance carbonation resistance, with the effect more pronounced and stable in BAS VPI systems. In mixes with additional SCMs like IS, the outcome is still generally positive but may be influenced by interactions between the SCM and SEA or the higher total binder content.

5.4.2. SEA effect on capillary absorption

In the BAS VPI system, the addition of SEA consistently reduced capillary absorption across all w/b ratios investigated as seen in Figure 5-17. At each level of w/b, an increase in SEA dosage from 0% to 4% led to a noticeable decrease in k_{cap}. For instance, at a w/b ratio of 0,4, the k_{cap} dropped from 0.0049 kg/m^2√s in the reference mix to 0,0042 kg/m^2√s with 2% SEA and further to 0,0036 kg/m^2√s with 4% SEA. A similar trend was evident at w/b 0,5 and 0,6, with reductions in k_{cap} from 0,0075 mm/√s to 0,0045 kg/m^2√s and from 0,0107 kg/m^2√s to 0,0066 kg/m^2√s, respectively, across the SEA dosage range. These results point to a strong relationship between SEA dosage and reduced capillary suction, suggesting that the admixture enhances the microstructural refinement of the cement structure. The reduction in k_{cap} values aligns with the understanding that SEA accelerates hydration, leading to the formation of a denser structure.

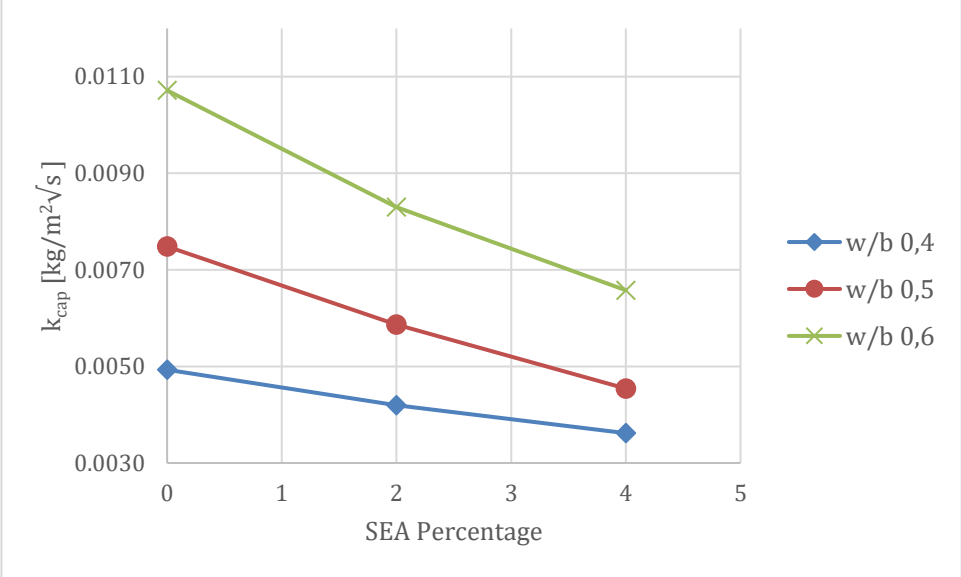

Figure 5-17 BAS VPI k_{cap} with Master X-Seed STE53. All values can be found in Appendix D1.

The m_{cap} also demonstrated a general improvement with increasing SEA dosage, particularly at lower w/b ratios as visualized in Figure 5-18. While some variation was observed at higher w/b, the values indicated an enhancement in resistance to capillary rise in the presence of SEA. Furthermore, active porosity followed a declining trend with the addition of SEA, see Figure 5-19, indicating a reduction in interconnected pore space that actively contributes to water transport. At w/b 0,5, for example, active porosity decreased from 11,15% to 9,99% as SEA content increased.

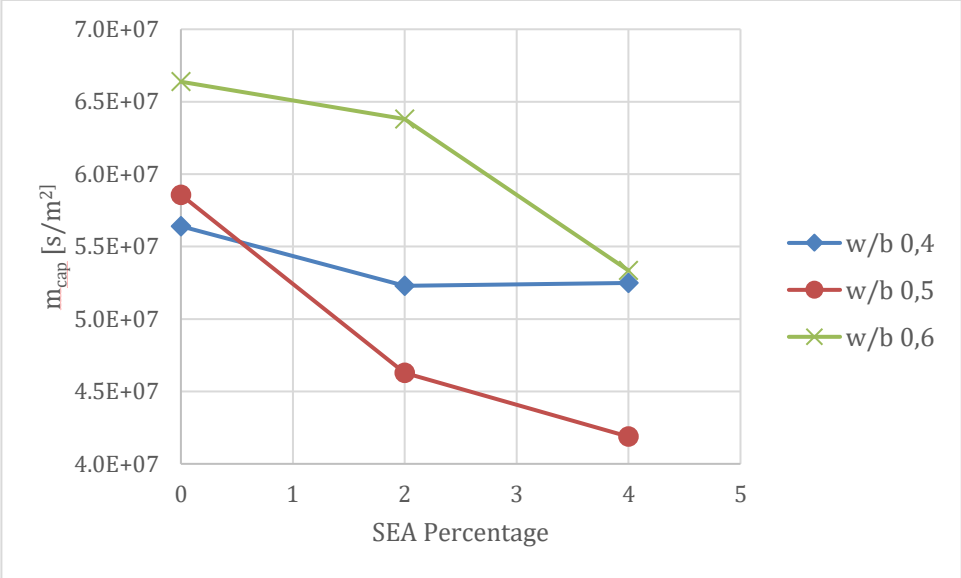

Figure 5-18 BAS VPI m_{cap} with Master X-Seed STE53. All values can be found in Appendix D1.

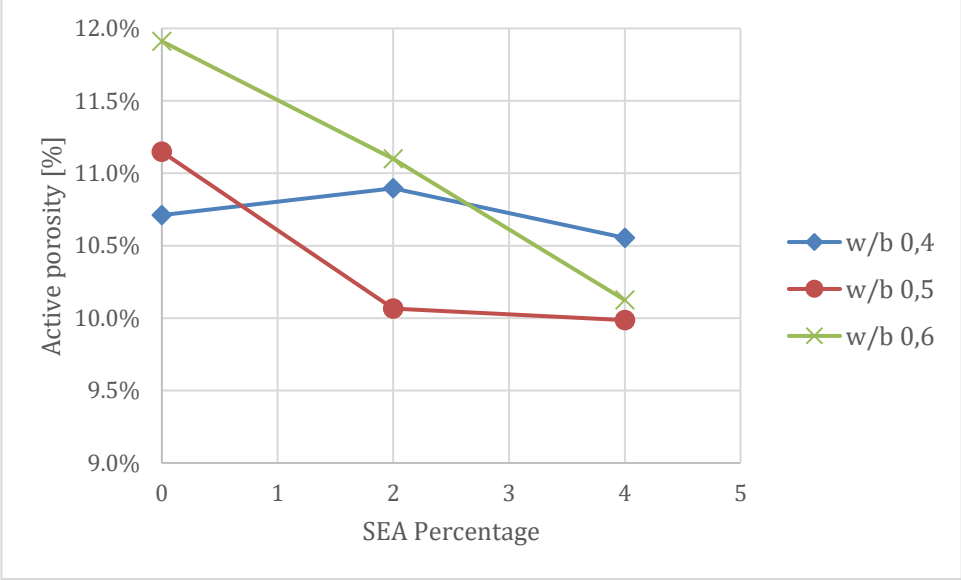

Figure 5-19 BAS VPI Active Porosity with Master X-Seed STE53. All values can be found in Appendix D1.

In contrast, the Akmenes 25% IS also showed a reduction in k_{cap} with increasing SEA dosage, though the trends were slightly less consistent, particularly at higher w/b ratios as shown in Figure 5-20. At w/b ratio 0,4 and 0,5, k_{cap} values decreased in a manner similar to that observed in the BAS VPI system. For example, at w/b 0,5, the k_{cap} declined from 0,0115 kg/m$^2\sqrt{s}$ in the reference to 0,0101 kg/m$^2\sqrt{s}$ and 0,0092 kg/m$^2\sqrt{s}$ with 2% and 4% SEA, respectively. However, at w/b = 0,6, the reduction in capillary absorption was more modest, suggesting that the beneficial effect of SEA may be less dominant when the porosity of the mix is higher.

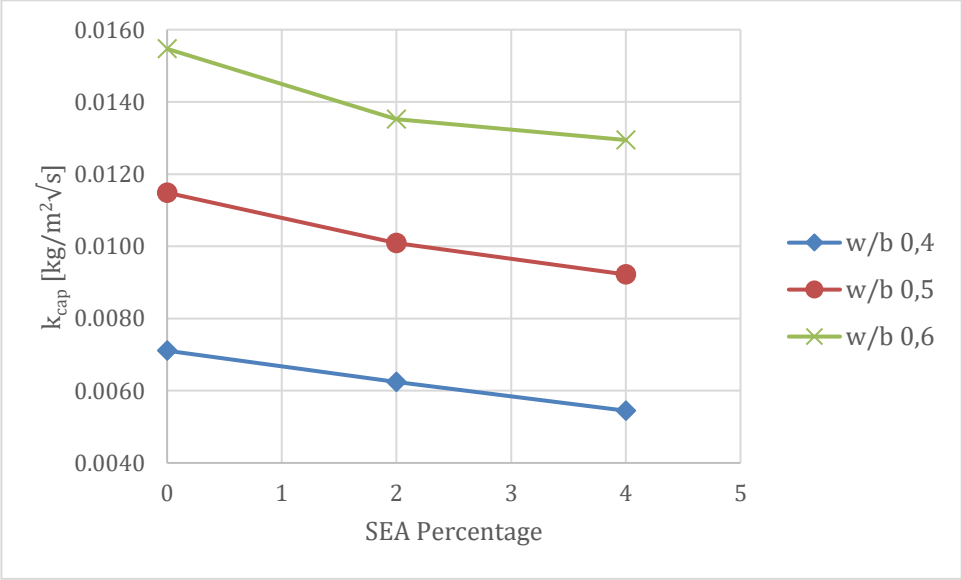

Figure 5-20 Akmenes 25% IS k_{cap} with Master X-Seed STE53. All values can be found in Appendix D2.

The behavior of m_{cap} in the Akmenes system was similarly varied. While some improvement in resistance was noted at lower w/b ratios, higher w/b mixes showed relatively stable or fluctuating values as shown in Figure 5-21, reflecting the complex interaction between the SEA, the SCMs, and the pore structure in these systems. Active porosity in the Akmenes mixes generally decreased with increasing SEA dosage as seen in Figure 5-22, especially at w/b 0,4 and 0,5, reinforcing the trend observed in the BAS VPI mixes. However, at w/b ratio 0,6, showed inconsistent results, with increasing SEA dosage increasing the active porosity.

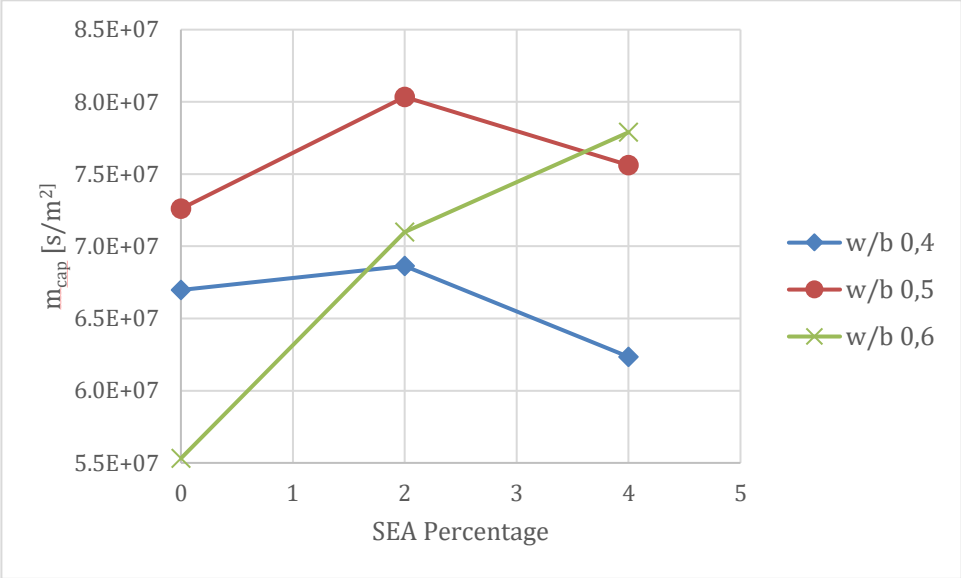

Figure 5-21 m_{cap} for Akmenes 25% IS with Master X-Seed STE53. All values can be found in Appendix D2.

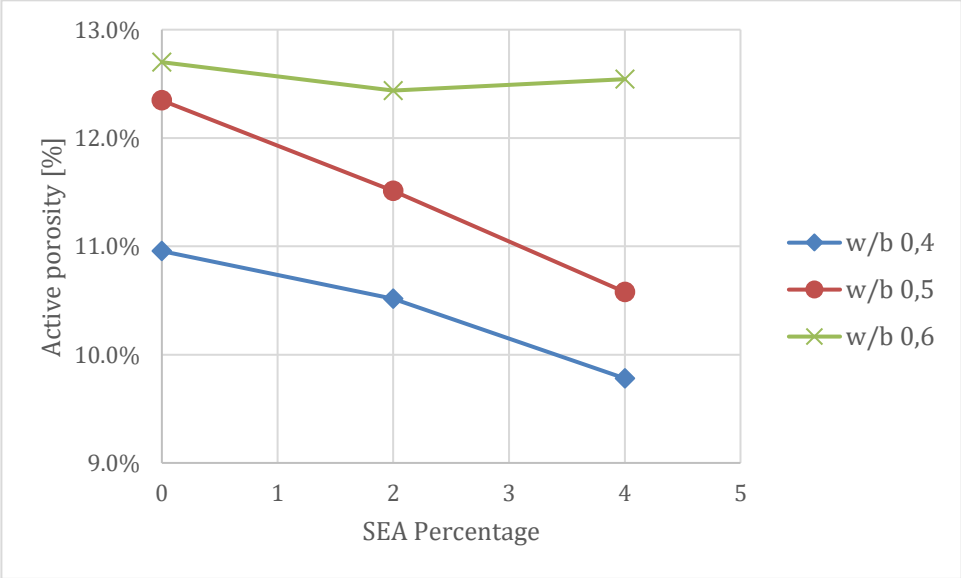

Figure 5-22 Active Porosity for Akmenes 25% IS with Master X-Seed STE53. All values can be found in Appendix D2.

Overall, the findings suggest that the inclusion of Master X-Seed STE53 enhances resistance to capillary water ingress by refining the pore network and reducing the active transport pathways. This effect is more consistent and pronounced in the BAS VPI system, particularly at lower w/b ratios. However, as evident in Figure 5-16 and Figure 5-19, the type of SCM also factors in the quantity of the effect. With the addition of IS, the improvement remains evident but may be moderated by the complexity of binder interactions and higher porosities.

Nevertheless, although the results from both systems indicate that increasing SEA dosage tends to improve capillary transport properties, evident from reductions in k_{cap}, m_{cap}, and active porosity, the sample size remains limited, and the trends observed cannot yet be regarded as conclusive. Furthermore, the data does not allow for clear identification of an optimal SEA dosage, as this may vary depending on the specific cement and SCM combinations used. Despite these limitations, the overall influence of SEA addition appears to be positive in lower w/b ratios, supporting its potential role in enhancing the capillary-related durability performance of concrete.

5.4.3. SEA effect on compressive strength

Figure 5-23 shows that in the BAS VPI system, a consistent improvement in compressive strength was observed with increasing SEA percentage at w/b ratios of 0,5 and 0,6. At w/b 0,5, strength increased from 54,05 MPa (0% SEA) to 65,56 MPa (4% SEA), indicating an effective response to SEA addition. Similarly, at w/b 0,6, compressive strength improved from 46,34 MPa to 52,02 MPa with 4% SEA. This suggests that SEA dosage contributed positively to the hydration process, enhancing continued strength development over time.

However, at w/b 0,4, while an increase was also observed with 4% SEA (from 57,55 MPa to 78,95 MPa), the 56-day strength of the control mix (0% SEA) was unexpectedly lower than its 28-day strength as seen in Figure 5-24. This anomaly, where 28-day strength exceeded 56-day strength, could be attributed to measurement variability, curing- or compacting inconsistencies. Despite this irregularity, the mix with 4% SEA achieved the highest strength among all BAS VPI samples.

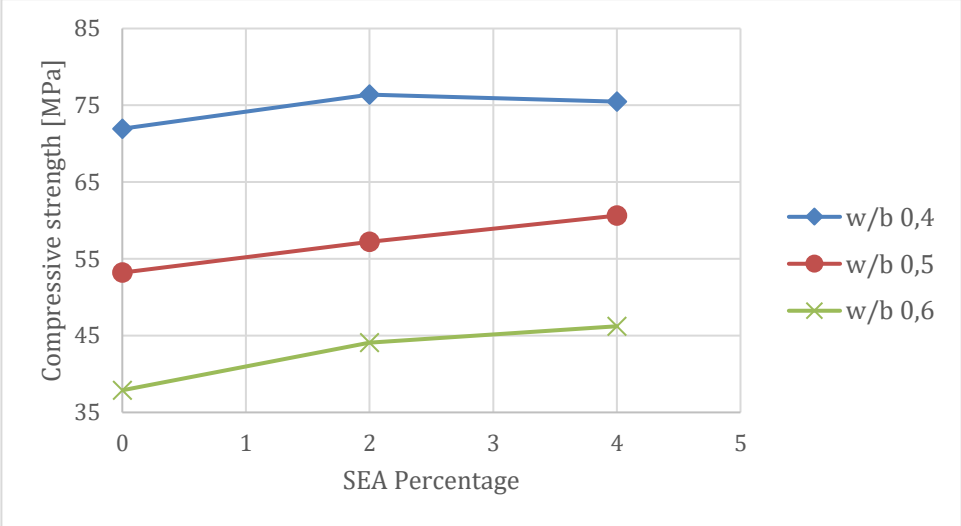

Figure 5-23 BAS VPI 28 days compressive strength with Master X-Seed STE53. All values can be found in Appendix D3.

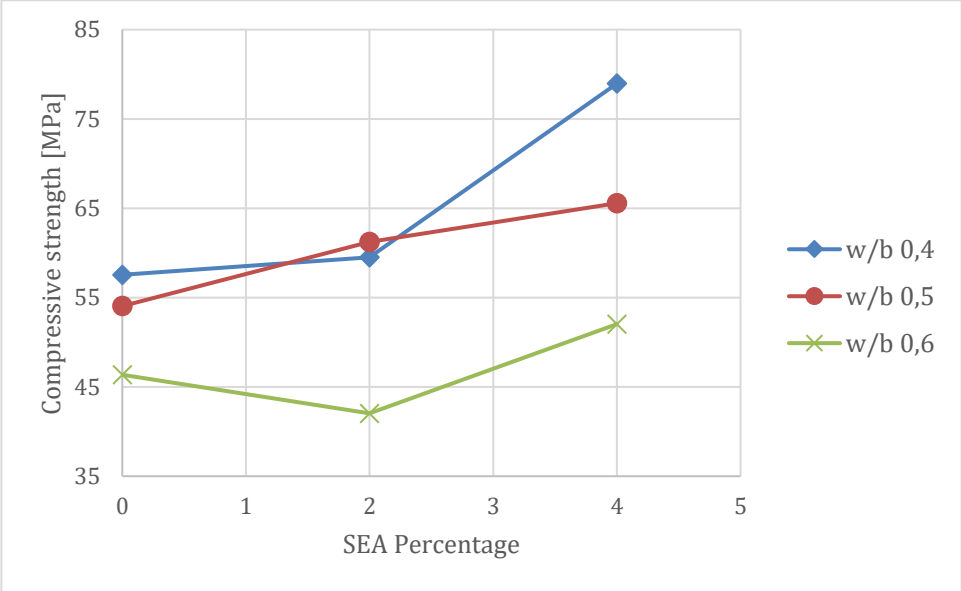

Figure 5-24 BAS VPI 56 days compressive strength with Master X-Seed STE53. All values can be found in Appendix D3.

Figure 5-25 shows that similar strength enhancement trends being noted for the Akmenes 25% IS system for 28 days. At w/b 0,4, compressive strength rose steadily from 57,6 MPa (0% SEA) to 61,6 MPa (4% SEA), with the 2% SEA mix reaching the highest strength (64,3 MPa). At w/b 0,5 and 0,6, strength also increased progressively with higher SEA dosage, although the gains were relatively smaller. For example, at w/b 0,6, the control mix had a strength of 28,1 MPa, improving to 34,3 MPa at 4% SEA.

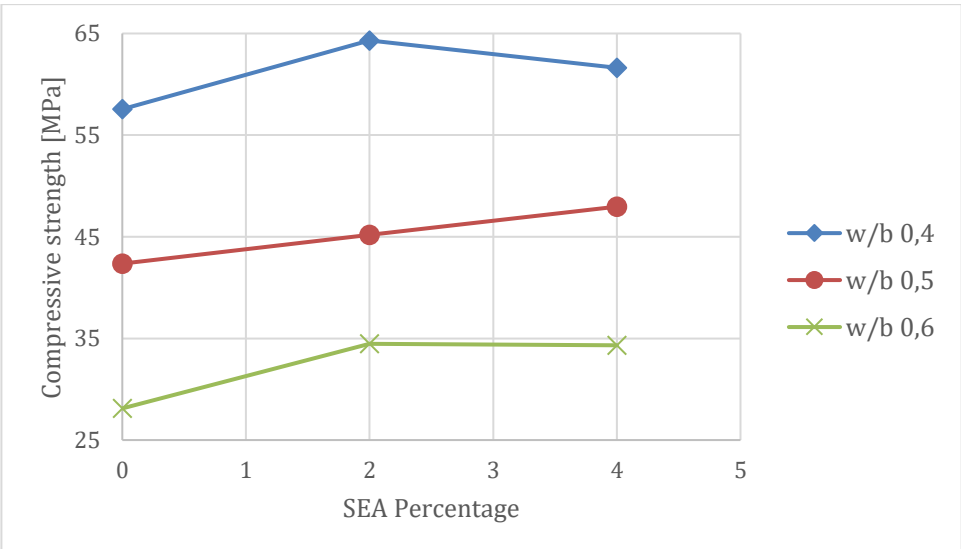

Figure 5-25 Akmenes 25% IS 28 days compressive strength with Master X-Seed STE53. All values can be found in Appendix D4.

56 day compressive strength results for Akmenes 25% IS systems follows the same trends as 28 day results, as seen in Figure 5-26. At w/b 0,4, compressive strength rose steadily from 60,55 MPa (0% SEA) to 70,39 MPa (4% SEA), with the 2% SEA mix reaching the highest strength (71,81 MPa). At w/b 0,5 and 0,6, strength also increased progressively with higher SEA dosage, although the gains were relatively smaller. For example, at w/b 0,6, the control mix had a strength of 32,88 MPa, improving to 39,24 MPa at 4% SEA.

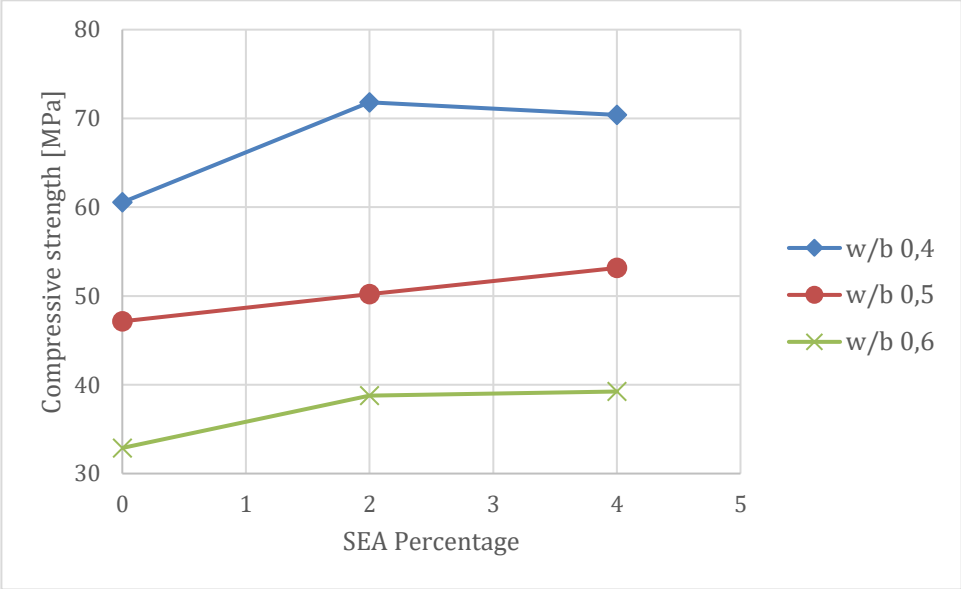

Figure 5-26 Akmenes 25% IS 56 days compressive strength with Master X-Seed STE53. All values can be found in Appendix D4.

While these results collectively demonstrate a positive effect of Master X-Seed STE53 on later-age strength in both systems, the data also highlights minor anomalies and non-linearities. These suggest that while SEA addition tends to enhance strength, the optimal dosage may depend on the binder type, SCM content, and w/b ratio. Moreover, the limited sample size restricts definitive conclusions. Nonetheless, the observed patterns highlights SEA's potential in boosting strength development, particularly in SCM mixed cementitious systems with lower early-age reactivity.

5.5. Comparison of SEAs

To evaluate the effect of admixture type on carbonation resistance, a direct comparison was made between mixes containing 4% Master X-Seed STE53 and 4% Master X-Seed 100, using the BAS VPI cementitious system across three different w/b ratios. Refer to Figure 5-27 for the carbonation coefficient values.

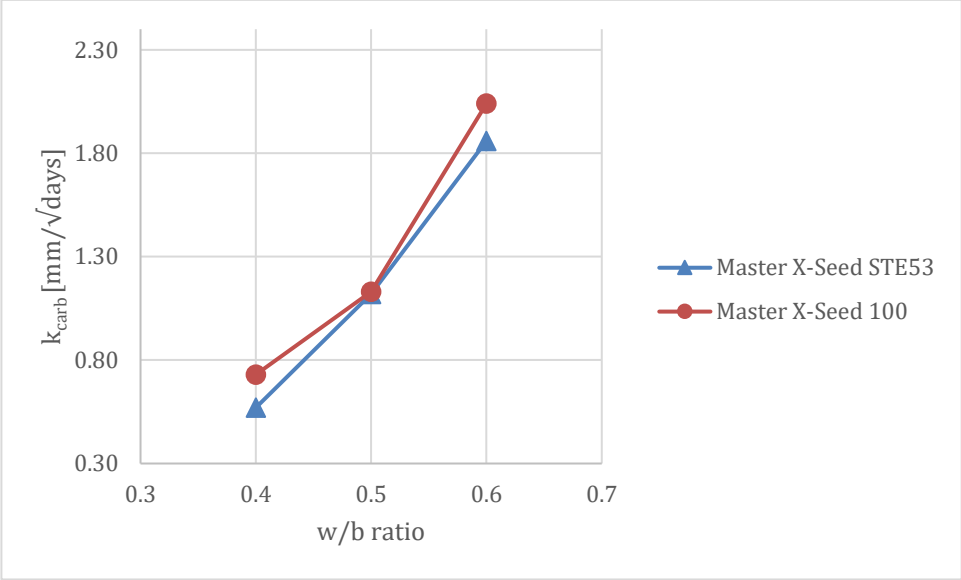

Figure 5-27 Carbonation of Master X-Seed 100 vs Master X-Seed STE53. All k_{carb} values can be found in Appendix B1.

At w/b 0,4, the mix with 4% Master X-Seed STE53 exhibited a carbonation coefficient of 0,57 mm/√days, while the mix with 4% Master X-Seed 100 showed a higher value of 0,73 mm/√days. This trend continued at w/b 0,5 and 0,6, where the Master X-Seed STE53 mixes consistently resulted in lower carbonation coefficients compared to the corresponding Master X-Seed 100 mixes (1,12 vs. 1,13 mm/√days at w/b 0,5, and 1,86 vs. 2,04 mm/√days at w/b 0,6).

While the differences at w/b 0,5 were minor, the gap was more noticeable at lower and higher w/b ratios, suggesting that Master X-Seed STE53 may be slightly more effective in improving carbonation resistance, particularly in leaner and more porous mixes. This may be attributed to differences in the seeding technology or solid content quantities or the type of superplasticizer used in the two admixtures, affecting the hydration procedure and resulting microstructure.

However, the number of results related to Master X-Seed 100 are minimal, thus preventing us from building a clearer case for its effect on carbonation and for drawing a more robust comparison with Master X-Seed STE53. Further testing across more mixes and cement systems would be needed for a conclusive assessment.

6. Conclusions

The relationship between carbonation and compressive strength

A general trend of inverse correlation was observed between carbonation resistance and compressive strength across all the tested concretes. Mixes with higher compressive strength typically exhibited lower carbonation coefficients, particularly at lower w/b ratios. For instance, at w/b 0,4, the BAS VPI concrete with 4% Master X-Seed STE53 reached a 56-day strength of 79 MPa and a relatively low carbonation coefficient of 0,57 mm/√days. In contrast, the Akmenes cement mix with 25% IS and 2% SEA at w/b 0,6 displayed the lowest strength (38,8 MPa at 56 days) and the highest carbonation coefficient (2,85 mm/√days), with full carbonation observed after 54 days.

The correlation between compressive strength and carbonation was strong for both BAS VPI and Akmenes mixes. Regression analyses for each cement and test period showed high R^2 values between 0,95 and 0,97, except for BAS VPI at 56 days, which had a lower R^2 value of 0,86. This was due to inconsistencies in the compressive strength results for w/b 0,4, as the mixes with no SEA and 2% Master X-Seed STE53 decreased in strength.

The relationship between carbonation and capillary absorption

The analysis revealed a positive correlation between the k_{cap} and the k_{carb}, particularly for concretes with consistent SCM and SEA content. In most mixes, higher k_{cap} values coincided with increased k_{carb} values, supporting the expectation that greater capillary porosity facilitates CO_2 ingress and accelerates carbonation. For instance, mixes with lower k_{cap} values, such as BAS VPI with 4% Master X-Seed STE53 at w/b 0,5, showed reduced carbonation depths compared to mixes with higher k_{cap} values like those of Akmenes cement with 25% IS and no SEA. The correlation between k_{carb} and k_{cap} increased with increased w/b ratio, as ratio 0,4 had a relatively high R^2 value of 0,82 while ratio 0,6 it reached 0,94, indicating that the correlation is almost linear.

SEA effect on Carbonation

SEAs are shown to have a positive impact on the carbonation in concretes utilizing SCMs. It was shown during the thesis work that for almost all concrete mixes, the carbonation coefficient decreased with an increased amount of SEA. The only mixes for which this wasn't the case was for Akmenes cement with 25% IS and 2% Master X-SEED STE53 and a w/b ratio of 0,6, where the carbonation coefficient increased by 0,03 mm/√days, and BAS VPI with 4% Master X-SEED 100 and a w/b ratio of 0,4, where the carbonation coefficient increased by 0,05 mm/√days.

The SEA that had the biggest impact on the carbonation coefficient was Master X-Seed STE53, which when compared to Master X-Seed 100 yielded greater decreases in carbonation coefficients compared to the case with no SEA for all w/b ratios.

SEA effect on Capillary Absorption

The incorporation of Master X-Seed STE53 demonstrated a generally positive influence on capillary absorption properties across both BAS VPI and Akmenes binder systems. A

consistent trend was observed where increasing the SEA dosage from 0% to 4% led to a reduction in k_{cap} suggesting enhanced resistance to moisture ingress. This effect was more pronounced in the BAS VPI mixes compared to Akmenes mixes. There could have been several reasons for this. The BAS VPI binder system, which contains volcanic pozzolan and limestone, may have benefitted additionally from the physical and chemical contributions of limestone. As a fine filler, limestone can help refine the pore structure, and in combination with SEA-driven hydration acceleration it might be showing consistent and higher capillary resistance.

In the Akmenes mixes containing 25% IS, the trends were generally similar, though less consistent. While increased SEA dosage led to reductions in k_{cap} and porosity, particularly at w/b ratios of 0,4 and 0,5, the effect was less evident at w/b 0,6. The higher water content might have improved the porosity which in return could have been a critical factor compared to the accelerated hydration due to SEA addition.

SEA effect on Compressive Strength

The addition of SEA had a generally positive influence on compressive strength development in both BAS VPI and Akmenes systems. In BAS VPI mixes, increasing SEA dosage from 0% to 4% led to improved strength at both 28 and 56 days, with the most consistent gains observed at w/b 0,5 and 0,6. At w/b 0,4, while the 28-day strength increased with SEA, the 56-day strength of the 2% mix remained close to the reference, and the 4% mix showed a notable increase, highlighting the delayed strength enhancement at higher dosage.

For Akmenes mixes containing 25% IS, SEA addition also contributed to strength gains, particularly at lower w/b ratios. However, at w/b 0,6, the strength values for all mixes remained relatively low, and the improvements from SEA were modest. This may reflect the higher porosity and lower reactivity at elevated w/b ratios, which can limit the efficiency of SEA.

Some anomalies were observed, for instance, in BAS VPI w/b 0.6 with 2% SEA, the 56-day strength slightly decreased compared to 28 days. Nonetheless, the overall trend indicates that SEA enhances strength development, with the extent of improvement influenced by binder type, SEA dosage, and w/b ratio.

Comparison of the two SEAs

The comparison between the two SEAs Master X-Seed STE53 and Master X-Seed 100 at 4% suggested that Master X-Seed STE53 offers slightly better carbonation resistance. At all three w/b ratios, the k_{carb} values were consistently lower for mixes incorporating STE53, with the difference more visible at w/b 0.4 and 0.6. This trend indicates that STE53 may perform more effectively in denser as well as more porous matrices, potentially due to differences in seeding characteristics, solid content quantities or the type of superplasticizer used in the two SEAs.

Limitations, future studies and final words

There were several limitations that affected the scope and depth of this study's statistical and comparative analyses. One of the main constraints was the limited use of Master X-Seed 100. This admixture was incorporated only at a single dosage level of 4% in the tested mixes. As a result, it was not possible to perform a meaningful analysis on the influence of Master X-Seed 100 across different dosages on carbonation resistance, capillary absorption, or compressive strength. Consequently, conclusions regarding its performance remain indicative and cannot be effectively compared to the trends observed for Master X-Seed STE53.

Another significant limitation was the availability of only single average values for each mix parameter. This limited the range of statistical tools that could be applied. For instance, ANOVA testing, which requires multiple data values per group, could not be conducted. The analysis had to rely primarily on correlation and linear regression methods, which, although informative, do not offer the same level of statistical strength.

Moreover, the overall sample size per binder system and admixture configuration was relatively small. This reduced the statistical power of the findings. Despite that, the observed trends such as the improvement in carbonation resistance and strength with increasing SEA dosage, align well with theoretical expectations and prior research, suggesting that the results are reasonable despite these constraints.

Future research is encouraged to address these limitations by incorporating a wider range of SEA dosages (particularly for Master X-Seed 100), including replicates to enable more advanced statistical analyses, and expanding the sample size across different binder and SCM combinations. Also, as evident throughout the study, the two selected SCMs work in different efficiency under different conditions. It will be practical to carry out studies separately for these two SCMs. Such work would help to more precisely identify the optimum level of SEA inclusion in SCM-containing cementitious systems in terms of both durability and mechanical performance.

7. References

[1] V.G. Papadakis, C.G. Vayenas, M.N. Fardis, Fundamental Modeling and Experimental Investigation of Concrete Carbonation, (n.d.). https://www.concrete.org/publications/internationalconcreteabstractsportal.aspx?m=details&ID=1863 (accessed September 30, 2025).

[2] P.K. Mehta, P.J.M. Monteiro, Concrete: Microstructure, Properties, and Materials, 4th Edition, McGraw-Hill Education, 2014. https://www.accessengineeringlibrary.com/content/book/9780071797870 (accessed June 5, 2025).

[3] V.T. Ngala, C.L. Page, EFFECTS OF CARBONATION ON PORE STRUCTURE AND DIFFUSIONAL PROPERTIES OF HYDRATED CEMENT PASTES, Cem. Concr. Res. 27 (1997) 995–1007. https://doi.org/10.1016/S0008-8846(97)00102-6.

[4] J. Justs, M. Wyrzykowski, D. Bajare, P. Lura, Internal curing by superabsorbent polymers in ultra-high performance concrete, Cem. Concr. Res. 76 (2015) 82–90. https://doi.org/10.1016/j.cemconres.2015.05.005.

[5] M. Thomas, Chloride thresholds in marine concrete, Cem. Concr. Res. 26 (1996). https://doi.org/10.1016/0008-8846(96)00035-X.

[6] J.A. Farny, B. Kerkhoff, Concrete Technology: Diagnosis and Control of Alkali-Aggregate Reactions in Concrete, 2007. https://trid.trb.org/View/813905 (accessed June 9, 2025).

[7] Properties of Concrete [5 ed.] 0273755803, 9780273755807, Dokumen.Pub (n.d.). https://dokumen.pub/properties-of-concrete-5nbsped-0273755803-9780273755807.html (accessed June 9, 2025).

[8] 7 Hydration of Portland cement, in: Cem. Chem., Thomas Telford Publishing, 1997: pp. 187–225. https://doi.org/10.1680/cc.25929.0007.

[9] M. Thomas, Supplementary Cementing Materials in Concrete, CRC Press, Boca Raton, 2013. https://doi.org/10.1201/b14493.

[10] Corrosion of Steel in Concrete Prevention Diagnosis Repair 1st Edition Luca Bertolini 2024 scribd download | PDF | Cement | Porosity, Scribd (n.d.). https://www.scribd.com/document/830942471/Corrosion-of-Steel-in-Concrete-Prevention-Diagnosis-Repair-1st-Edition-Luca-Bertolini-2024-scribd-download (accessed June 9, 2025).

[11] Saetta and Vitaliani - 2004 - Experimental Investigation and Numerical Modeling | PDF, Scribd (n.d.). https://www.scribd.com/document/775645455/Saetta-and-Vitaliani-2004-Experimental-investigation-and-numerical-modeling (accessed June 9, 2025).

[12] K. Tuutti, CORROSION OF STEEL IN CONCRETE, CBI ForskResearch (1982). https://trid.trb.org/View/194388 (accessed June 9, 2025).

[13] G. Gluth, X. Ke, A. Vollpracht, L. Weiler, S.A. Bernal, M. Cyr, K. Dombrowski-Daube, D.A. Geddes, C. Grengg, C. Le Galliard, M. Nedeljkovic, J.L. Provis, L. Valentini, B. Walkley, Carbonation rate of alkali-activated concretes and high-volume SCM concretes: a literature data analysis by RILEM TC 281-CCC, Mater. Struct. 55 (2022). https://doi.org/10.1617/s11527-022-02041-4.

[14] K. Sisomphon, L. Franke, Carbonation rates of concretes containing high volume of pozzolanic materials, Cem. Concr. Res. 37 (2007) 1647–1653. https://doi.org/10.1016/j.cemconres.2007.08.014.

[15] J. Wang, T. Lord, Y. Wang, L. Black, Q. Li, Effects of carbonation on mechanical properties of concrete under high temperature and impact, Inst. Civ. Eng. Proc. Smart Infrastruct. Constr. 175 (2022) 44–56. https://doi.org/10.1680/jsmic.21.00021.
[16] Carbonation of concrete, Concr. Cent. (n.d.). https://www.concretecentre.com/Performance-Sustainability/Whole-life-carbon/Carbonation-of-concrete.aspx (accessed June 9, 2025).
[17] Correlation between initial absorption of the cover concrete, the compressive strength and carbonation depth | Request PDF, ResearchGate (n.d.). https://doi.org/10.1016/j.conbuildmat.2013.03.074.
[18] F. Pacheco-Torgal, J.A. Labrincha, C. Leonelli, A. Palomo, P. Chindaprasirt, eds., Front matter, in: Handb. Alkali-Act. Cem. Mortars Concr., Woodhead Publishing, Oxford, 2015: pp. i–iii. https://doi.org/10.1016/B978-1-78242-276-1.50029-0.
[19] S. von Greve-Dierfeld, B. Lothenbach, A. Vollpracht, B. Wu, B. Huet, C. Andrade, C. Medina, C. Thiel, E. Gruyaert, H. Vanoutrive, I.F. Saéz del Bosque, I. Ignjatovic, J. Elsen, J.L. Provis, K. Scrivener, K.-C. Thienel, K. Sideris, M. Zajac, N. Alderete, Ö. Cizer, P. Van den Heede, R.D. Hooton, S. Kamali-Bernard, S.A. Bernal, Z. Zhao, Z. Shi, N. De Belie, Understanding the carbonation of concrete with supplementary cementitious materials: a critical review by RILEM TC 281-CCC, Mater. Struct. 53 (2020) 136. https://doi.org/10.1617/s11527-020-01558-w.
[20] R. Firdous, D. Stephan, J.N.Y. Djobo, Natural pozzolan based geopolymers: A review on mechanical, microstructural and durability characteristics, Constr. Build. Mater. 190 (2018) 1251–1263. https://doi.org/10.1016/j.conbuildmat.2018.09.191.
[21] J. Brännland, A. Andersson, Hållfasthetsutveckling för betong med hög andel mineraliska tillsatsmaterial, 2023. https://urn.kb.se/resolve?urn=urn:nbn:se:uu:diva-511702 (accessed June 22, 2025).
[22] J.A. Suárez-Navarro, M.A. Sanjuán, C. Argiz, G. Hernáiz, M. Barragán, E. Estévez, Radiological assessment of iron silicate as a potential aggregate in concrete and mortars, Cem. Concr. Compos. 129 (2022) 104490. https://doi.org/10.1016/j.cemconcomp.2022.104490.
[23] C. Shi, C. Meyer, A. Behnood, Utilization of copper slag in cement and concrete, Resour. Conserv. Recycl. 52 (2008) 1115–1120. https://doi.org/10.1016/j.resconrec.2008.06.008.
[24] M. Mastali, A. Alzaza, K. Mohammad Shaad, P. Kinnunen, Z. Abdollahnejad, B. Woof, M. Illikainen, Using Carbonated BOF Slag Aggregates in Alkali-Activated Concretes, Materials 12 (2019) 1288. https://doi.org/10.3390/ma12081288.
[25] N. Kaid, M. Cyr, S. Julien, H. Khelafi, Durability of concrete containing a natural pozzolan as defined by a performance-based approach, Constr. Build. Mater. 23 (2009) 3457–3467. https://doi.org/10.1016/j.conbuildmat.2009.08.002.
[26] M.B. Haha, K. De Weerdt, B. Lothenbach, Quantification of the degree of reaction of fly ash, Cem. Concr. Res. 40 (2010) 1620–1629. https://doi.org/10.1016/j.cemconres.2010.07.004.
[27] Bascement Plus Slite | Heidelberg Materials Cement Sverige, (n.d.). https://www.cement.heidelbergmaterials.se/sv/bascement-plus-slite (accessed September 14, 2025).
[28] Cement types, Akmenės Cem. (n.d.). https://cementas.lt/en/production/cement-types/ (accessed July 7, 2025).

[29] A. Cuesta, A. Morales-Cantero, A.G. De la Torre, M.A.G. Aranda, Recent Advances in C-S-H Nucleation Seeding for Improving Cement Performances, Materials 16 (2023) 1462. https://doi.org/10.3390/ma16041462.
[30] D.T. Wu, Nucleation Theory, in: H. Ehrenreich, F. Spaepen (Eds.), Solid State Phys., Academic Press, 1996: pp. 37–187. https://doi.org/10.1016/S0081-1947(08)60604-9.
[31] Master X-Seed 100 - betongaccelerator, (n.d.). https://master-builders-solutions.com/sv-se/produkter/master-x-seed/masterx-seed-100/ (accessed June 26, 2025).
[32] Master X-Seed STE 53, (n.d.). https://master-builders-solutions.com/sv-se/produkter/master-x-seed/master-x-seed-ste-53/ (accessed June 26, 2025).
[33] I. Monteiro, F.A. Branco, J. de Brito, R. Neves, Statistical analysis of the carbonation coefficient in open air concrete structures, Constr. Build. Mater. 29 (2012) 263–269. https://doi.org/10.1016/j.conbuildmat.2011.10.028.
[34] J. Crank, The Mathematics of Diffusion, Oxford University Press, Oxford, 1976.
[35] S. Poyet, B. Bary, N. Seigneur, Effect of carbonation on the water retention of cementitious materials: case of a C–S–H paste (C/S = 1.4), Npj Mater. Degrad. 9 (2025) 46. https://doi.org/10.1038/s41529-025-00597-4.
[36] B. Kraft, R. Achenbach, H.-M. Ludwig, M. Raupach, Hydration and Carbonation of Alternative Binders, Corros. Mater. Degrad. 3 (2022) 19–52. https://doi.org/10.3390/cmd3010003.
[37] Applied statistics and probability for engineers, ResearchGate (n.d.). https://www.researchgate.net/publication/317415389_Applied_statistics_and_probability_for_engineers (accessed July 7, 2025).
[38] M. Stefanoni, U. Angst, B. Elsener, The mechanism controlling corrosion of steel in carbonated cementitious materials in wetting and drying exposure, Cem. Concr. Compos. 113 (2020) 103717. https://doi.org/10.1016/j.cemconcomp.2020.103717.

Appendices

Appendix A Compressive Strength Results

Appendix A1 Mean compressive strength results for 28 days and 56 days for BAS VPI mixes

Cement	SCM	SCM dosage [wt %]	w/b ratio	SEA	SEA dosage [wt %]	Compressive strength 28 days [MPa]	Compressive strength 56 days [MPa]
BAS VPI	VPI	30	0,4			72,0	57,5
BAS VPI	VPI	30	0,5			53,2	54,0
BAS VPI	VPI	30	0,6			37,9	46,3
BAS VPI	VPI	30	0,4	Master X-Seed STE53	2	76,4	59,5
BAS VPI	VPI	30	0,5	Master X-Seed STE53	2	57,2	61,2
BAS VPI	VPI	30	0,6	Master X-Seed STE53	2	44,1	42,0
BAS VPI	VPI	30	0,4	Master X-Seed STE53	4	75,5	79,0
BAS VPI	VPI	30	0,5	Master X-Seed STE53	4	60,6	65,6
BAS VPI	VPI	30	0,6	Master X-Seed STE53	4	46,2	52,0
BAS VPI	VPI	30	0,4	Master X-Seed 100	4	75,9	78,7
BAS VPI	VPI	30	0,5	Master X-Seed 100	4	60,7	65,5
BAS VPI	VPI	30	0,6	Master X-Seed 100	4	44,9	49,4
BAS VPI	VPI	30	0,4	Master X-Seed STE53	0,2	74,6	83,1

Appendix A2 Mean compressive strength results for 28 days and 56 days for Akmenes mixes

Cement	SCM	SCM dosage [wt %]	w/b ratio	SEA	SEA dosage [wt %]	Compressive strength 28 days [MPa]	Compressive strength 56 days [MPa]
Akmenes	Iron silicates	25	0,4			57,6	60,5
Akmenes	Iron silicates	25	0,5			42,4	47,1
Akmenes	Iron silicates	25	0,6			28,1	32,9
Akmenes	Iron silicates	25	0,4	Master X-Seed STE53	2	64,3	71,8
Akmenes	Iron silicates	25	0,5	Master X-Seed STE53	2	45,2	50,2
Akmenes	Iron silicates	25	0,6	Master X-Seed STE53	2	34,5	38,8
Akmenes	Iron silicates	25	0,4	Master X-Seed STE53	4	61,6	70,4
Akmenes	Iron silicates	25	0,5	Master X-Seed STE53	4	48,0	53,2
Akmenes	Iron silicates	25	0,6	Master X-Seed STE53	4	34,3	39,2
Akmenes	-----	0	0,4			60,0	64,8
Akmenes	-----	0	0,5			50,5	51,6
Akmenes	-----	0	0,6			40,7	42,6

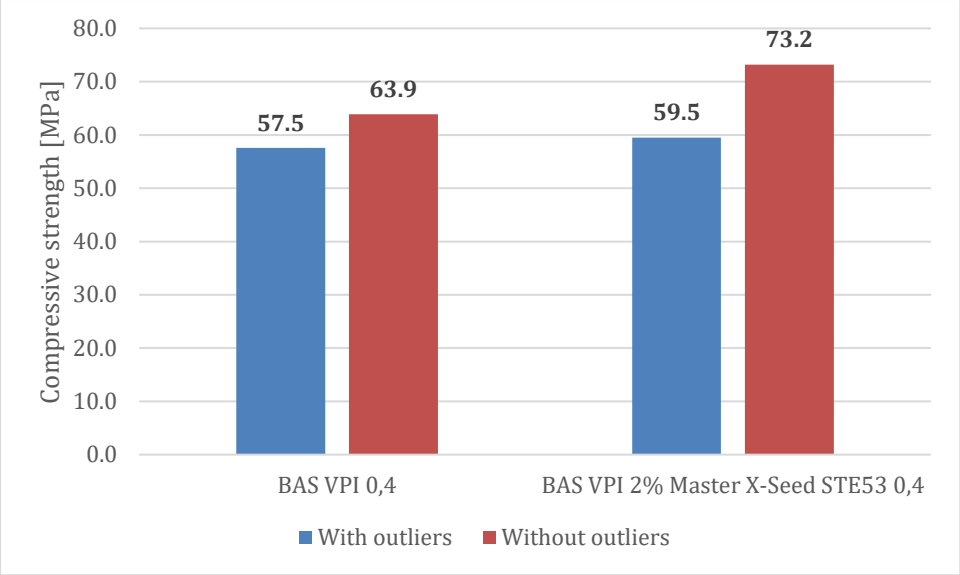

Appendix A3 56 days mean compressive strength for mixes with and without outliers

Appendix B Carbonation Depths and Coefficients

Appendix B1 Carbonation Depths and Coefficients for all mixes

Mix	Carbonation depth 14 days [mm]	Carbonation depth 28 days [mm]	Carbonation depth 40 days [mm]	Carbonation depth 54 days [mm]	Carbonation Coefficient [mm/√days]
BAS VPI 0,4	3,5	4,1	3,8	4,5	0,68
BAS VPI 0,5	5,1	6,6	8,3	9,8	1,31
BAS VPI 0,6	7,4	10,3	16,5	16,2	2,25
BAS VPI 2% Master X-SEED STE53 0,4	3,3	3,0	3,2	5,0	0,63
BAS VPI 2% Master X-SEED STE53 0,5	4,6	6,4	8,2	8,9	1,24
BAS VPI 2% Master X-SEED STE53 0,6	6,8	9,1	12,6	14,8	1,93
BAS VPI 4% Master X-SEED STE53 0,4	3,1	1,5	3,3	5,0	0,57
BAS VPI 4% Master X-SEED STE53 0,5	4,8	5,2	7,4	8,2	1,12
BAS VPI 4% Master X-SEED STE53 0,6	6,1	8,8	10,5	15,9	1,86
BAS VPI 4% Master X-SEED 100 0,4	2,7	2,8	4,9	5,9	0,73
BAS VPI 4% Master X-SEED 100 0,5	4,4	6,1	7,3	8,0	1,13
BAS VPI 4% Master X-SEED 100 0,6	6,9	9,2	13,6	15,8	2,04

Akmenes 25% IS 0,4	4,2	4,7	5,4	7,6	0,96
Akmenes 25% IS 0,5	7,6	9,1	14,7	19,6	2,30
Akmenes 25% IS 0,6	10,9	14,5	18,8	20,0	2,82
Akmenes 25% IS 2% Master X-SEED STE53 0,4	3,2	3,3	5,7	5,8	0,80
Akmenes 25% IS 2% Master X-SEED STE53 0,5	6,4	8,8	11,7	13,0	1,77
Akmenes 25% IS 2% Master X-SEED STE53 0,6	10,2	16,0	18,7	20,0	2,85
Akmenes 25% IS 4% Master X-SEED STE53 0,4	2,8	3,8	4,5	5,6	0,73
Akmenes 25% IS 4% Master X-SEED STE53 0,5	6,3	5,9	10,2	12,7	1,56
Akmenes 25% IS 4% Master X-SEED STE53 0,6	9,7	12,7	18,2	19,0	2,64
Akmenes 0,4	1,1	1,6	1,6	1,9	0,26
Akmenes 0,5	3,7	3,8	6,1	6,4	0,89
Akmenes 0,6	6,0	7,8	10,6	14,5	1,74
BAS VPI 0,2% Master X-SEED STE53 0,4	1,9	2,3	3,9	3,4	0,51

Appendix C Capillary Absorption Results

Appendix C1 w/b 0,4 capillary coefficient and resistance number

mix type	Qcap [kg/m$_2$]	$\sqrt{t_{cap}}$ [$\sqrt{s}$]	Capillary coefficient k_{cap} [kg/m$^2\sqrt{s}$]	Resistance number m_{cap} [s/m^2]
BAS VPI 0,4	0.75	151.2	0.0049	5.64E+07
BAS VPI 2% Master X-Seed STE53 0,4	0.62	148.5	0.0042	5.23E+07
BAS VPI 4% Master X-Seed STE53 0,4	0.53	147.1	0.0036	5.25E+07
BAS VPI 4% Master X-Seed 100 0,4	0.58	147.2	0.0040	5.10E+07
Akmenes 25% IS 0,4	1.20	169.1	0.0071	6.70E+07
Akmenes 25% IS 2% Master X-Seed STE53 0,4	1.08	173.7	0.0062	6.86E+07
Akmenes 25% IS 4% Master X-Seed STE53 0,4	0.89	163.4	0.0054	6.23E+07
Akmenes 0,4	1.18	163.2	0.0072	6.18E+07

Appendix C2 w/b 0,5 capillary coefficient and resistance number

mix type	Qcap [kg/m$_2$]	$\sqrt{t_{cap}}$ [$\sqrt{s}$]	Capillary coefficient k_{cap} [kg/m$^2\sqrt{s}$]	Resistance number m_{cap} [s/m^2]
BAS VPI 0,5	1.18	157.2	0.0075	5.86E+07
BAS VPI 2% Master X-Seed STE53 0,5	0.84	143.1	0.0059	4.63E+07
BAS VPI 4% Master X-Seed STE53 0,5	0.62	135.7	0.0045	4.19E+07
BAS VPI 4% Master X-Seed 100 0,5	0.75	139.5	0.0054	4.43E+07
Akmenes 25% IS 0,5	2.07	180.3	0.011	7.26E+07
Akmenes 25% IS 2% Master X-Seed STE53 0,5	1.93	191.8	0.010	8.03E+07
Akmenes 25% IS 4% Master X-Seed STE53 0,5	1.74	189.0	0.0092	7.56E+07
Akmenes 0,5	1.84	177.5	0.010	7.32E+07

Appendix C3 w/b 0,6 capillary coefficient and resistance number

mix type	Qcap [kg/m$_2$]	$\sqrt{t_{cap}}$ [$\sqrt{s}$]	Capillary coefficient k_{cap} [kg/m$^2\sqrt{s}$]	Resistance number m_{cap} [s/m^2]
BAS VPI 0,6	1.85	172.7	0.011	6.64E+07
BAS VPI 2% Master X-Seed STE53 0,6	1.39	167.2	0.0083	6.38E+07
BAS VPI 4% Master X-Seed STE53 0,6	1.00	152.2	0.0066	5.33E+07
BAS VPI 4% Master X-Seed 100 0,6	1.17	146.0	0.0080	4.83E+07
Akmenes 25% IS 0,6	2.41	155.9	0.015	5.53E+07
Akmenes 25% IS 2% Master X-Seed STE53 0,6	2.41	178.1	0.014	7.10E+07
Akmenes 25% IS 4% Master X-Seed STE53 0,6	2.41	186.5	0.013	7.79E+07
Akmenes 0,6	2.22	149.3	0.015	5.08E+07

Appendix C4 w/b 0,4 porosity results

mix type	Active porosity [%]	Total porosity [%]
BAS VPI 0,4	10.71	15.25
BAS VPI 2% Master X-Seed STE53 0,4	10.90	15.57
BAS VPI 4% Master X-Seed STE53 0,4	10.55	15.11
BAS VPI 4% Master X-Seed 100 0,4	10.85	14.97
Akmenes 25% IS 0,4	10.96	15.55
Akmenes 25% IS 2% Master X-Seed STE53 0,4	10.52	15.69
Akmenes 25% IS 4% Master X-Seed STE53 0,4	9.78	15.80
Akmenes 0,4	10.60	14.84

Appendix C5 w/b 0,5 porosity results

mix type	Active porosity [%]	Total porosity [%]
BAS VPI 0,5	11.15	16.39
BAS VPI 2% Master X-Seed STE53 0,5	10.06	15.55
BAS VPI 4% Master X-Seed STE53 0,5	9.99	15.82
BAS VPI 4% Master X-Seed 100 0,5	10.78	16.29
Akmenes 25% IS 0,5	12.35	16.13
Akmenes 25% IS 2% Master X-Seed STE53 0,5	11.51	16.05
Akmenes 25% IS 4% Master X-Seed STE53 0,5	10.58	16.15
Akmenes 0,5	11.84	15.55

Appendix C6 w/b 0,6 porosity results

mix type	Active porosity [%]	Total porosity [%]
BAS VPI 0,6	11.91	16.79
BAS VPI 2% Master X-Seed STE53 0,6	11.10	17.04
BAS VPI 4% Master X-Seed STE53 0,6	10.13	17.21
BAS VPI 4% Master X-Seed 100 0,6	10.69	16.76
Akmenes 25% IS 0,6	12.70	16.23
Akmenes 25% IS 2% Master X-Seed STE53 0,6	12.44	16.52
Akmenes 25% IS 4% Master X-Seed STE53 0,6	12.54	17.04
Akmenes 0,6	12.43	15.73

Appendix D Results Analysis with increasing Dosage

Appendix D1 BAS VPI Capillary Absorption Analysis with increasing SEA Dosage

Mix type	SEA %	k_{cap} [kg/m2√s]	m_{cap} [s/m2]	Active Porosity [%]	Total Porosity [%]
BAS VPI 0,4	0	0.0049	5.6E+07	10.71	15.25
BAS VPI 2% Master X-Seed STE53 0,4	2	0.0042	5.2E+07	10.90	15.57
BAS VPI 4% Master X-Seed STE53 0,4	4	0.0036	5.2E+07	10.55	15.11
BAS VPI 0,5	0	0.0075	5.9E+07	11.15	16.39
BAS VPI 2% Master X-Seed STE53 0,5	2	0.0059	4.6E+07	10.06	15.55
BAS VPI 4% Master X-Seed STE53 0,5	4	0.0045	4.2E+07	9.99	15.82
BAS VPI 0,6	0	0.0107	6.6E+07	11.91	16.79
BAS VPI 2% Master X-Seed STE53 0,6	2	0.0083	6.4E+07	11.10	17.04
BAS VPI 4% Master X-Seed STE53 0,6	4	0.0066	5.3E+07	10.13	17.21

Appendix D2 Akmenes Capillary Absorption Analysis with increasing SEA Dosage

Mix Type	SEA %	k_{cap} [kg/m2√s]	m_{cap} [s/m2]	Active Porosity [%]	Total Porosity [%]
Akmenes 25% IS 0,4	0	0.0071	6.7E+07	10.96	15.55
Akmenes 25% IS 2% Master X-Seed STE53 0,4	2	0.0062	6.9E+07	10.52	15.69
Akmenes 25% IS 4% Master X-Seed STE53 0,4	4	0.0054	6.2E+07	9.78	15.80
Akmenes 25% IS 0,5	0	0.0115	7.3E+07	12.35	16.13
Akmenes 25% IS 2% Master X-Seed STE53 0,5	2	0.0101	8.0E+07	11.51	16.05
Akmenes 25% IS 4% Master X-Seed STE53 0,5	4	0.0092	7.6E+07	10.58	16.15
Akmenes 25% IS 0,6	0	0.0155	5.5E+07	12.70	16.23
Akmenes 25% IS 2% Master X-Seed STE53 0,6	2	0.0135	7.1E+07	12.44	16.52
Akmenes 25% IS 4% Master X-Seed STE53 0,6	4	0.0129	7.8E+07	12.54	17.04

Appendix D3 BAS VPI Compressive Strength Analysis with increasing SEA Dosage

Mix type	SEA %	Compressive Strength 28d [MPa]	Compressive Strength 56d [MPa]
BAS VPI 0,4	0	72.0	57.5
BAS VPI 2% Master X-Seed STE53 0,4	2	76.4	59.5
BAS VPI 4% Master X-Seed STE53 0,4	4	75.5	79,0
BAS VPI 0,5	0	53.2	54.0
BAS VPI 2% Master X-Seed STE53 0,5	2	57.2	61.2
BAS VPI 4% Master X-Seed STE53 0,5	4	60.6	65.6
BAS VPI 0,6	0	37.9	46.3
BAS VPI 2% Master X-Seed STE53 0,6	2	44.1	42.0
BAS VPI 4% Master X-Seed STE53 0,6	4	46.2	52.0

Appendix D4 Akmenes Compressive Strength Analysis with increasing SEA Dosage

Mix type	SEA %	Compressive Strength 28d [MPa]	Compressive Strength 56d [MPa]
Akmenes 25% IS 0,4	0	57.6	60.5
Akmenes 25% IS 2% Master X-Seed STE53 0,4	2	64.3	71.8
Akmenes 25% IS 4% Master X-Seed STE53 0,4	4	61.6	70.4
Akmenes 25% IS 0,5	0	42.4	47.1
Akmenes 25% IS 2% Master X-Seed STE53 0,5	2	45.2	50.2
Akmenes 25% IS 4% Master X-Seed STE53 0,5	4	48,0	53.2
Akmenes 25% IS 0,6	0	28.1	32.9
Akmenes 25% IS 2% Master X-Seed STE53 0,6	2	34.5	38.8
Akmenes 25% IS 4% Master X-Seed STE53 0,6	4	34.3	39.2